RE-EXAMINING TROPICAL CYCLONE RADIAL STRUCTURE FROM FLIGHT-LEVEL AIRCRAFT OBSERVATIONS: IMPLICATIONS FOR VORTEX RESILIENCY AND INTENSIFICATION

A THESIS SUBMITTED TO THE GRADUATE DIVISION OF THE UNIVERSITY OF HAWAI'I IN PARTIAL FULFILLMENT OF THE REQUIREMENTS FOR THE DEGREE OF

MASTER OF SCIENCE

IN

METEOROLOGY

MAY 2004

By
Kevin J. Mallen

Thesis Committee:

Bin Wang, Chairperson
Gary Barnes
Yuqing Wang
Michael T. Montgomery

ABSTRACT

The importance of the radial structure on two aspects of the tropical cyclone (TC) intensity change problem is addressed: the vortex resiliency to ambient vertical wind shear and rapid vortex intensification. Theoretical studies, based on vortex Rossby wave (VRW) dynamics, have established that the degree of *vortex broadness* in the near-core region beyond the radius of maximum wind (RMW) determines the realignment or tilting over of a TC vortex in vertically sheared environments. The sensitivity of the initial specification of idealized vortices demonstrated by numerical simulations brings into question how well the "true" nature of TC radial structure is represented by some commonly used idealized vortices. Although the importance of the initial radial structure on the rate of vortex intensification is not well established theoretically, the issue of whether unique aspects of the swirling wind structure are observed prior to rapid intensification events is also addressed.

The primary circulation of TCs is re-examined by utilizing flight-level observations collected from Atlantic and eastern Pacific storms during 1977-2001, in which several hundred radial profiles of azimuthal-

mean tangential wind and relative vorticity are constructed from over five thousand flight leg segments. This comprehensive analysis principally reaffirms that real TC structure is characterized by a relatively slow tangential wind decrease beyond the RMW and a monotonically decreasing *skirt of significant cyclonic relative vorticity*. These characteristics, however, are found to be conspicuously absent in some idealized vortices frequently used in theoretical studies of TC evolution. Secondly, an investigation of the relationship between the initial tangential wind structure and the future intensification rate reveals that no *unique* characteristics exist just prior to rapid intensification events. The restricted range observed in the tangential wind parameters for a limited number of cases, however, suggest that *necessary* conditions may exist for rapid intensification. Although the radial structure appears to be critical for the vortex resiliency, the sole importance of the initial swirling wind structure on the intensification remains inconclusive.

TABLE OF CONTENTS

LIST OF TABLES

LIST OF FIGURES

CHAPTER 1. INTRODUCTION

1.1. Motivation

In the field of tropical cyclone (TC) research, recent years have seen a shift in emphasis from the study of the storm motion to a focus on the vortex *intensity*. This is in part a consequence of the continued lack of skill demonstrated in the operational forecasting of TC intensity changes, in contrast to the significant improvement seen in the track forecast. One particular scenario in which intensity forecasting lacks considerable skill is when TC vortices are embedded in vertically sheared environments (DeMaria and Kaplan 1994, 1999). Even in the absence of strong vertical shear, unexpected rapid intensity changes (e.g., hurricane Opal in 1995) typically result in large forecast errors.

The inability to forecast intensity change clearly reflects an inadequate physical understanding of the problem and demonstrates the need to improve the statistical and dynamical models that are used as forecasting guidance. A key to improved performance of dynamical models (in addition to other factors), is the accurate specification of the initial vortex structure (Kurihara et al. 1998). For example, the rapid intensification of hurricane Gloria (1985) was predicted by the GFDL

hurricane model after a more realistic initial vortex was specified (Bender et al. 1993). The lack of skill exhibited by statistical models which incorporate only environmental predictors, and not those based on internal dynamics, may be further evidence of the importance of the vortex structure.

The focus of this thesis will thus concern the importance of the initial azimuthal-mean TC radial structure on its evolution with respect to two important aspects of the intensity change problem: 1) the vortex response to environmental vertical wind shear and 2) rapid intensification. The next two sections discuss the specific motivation and background theory related to these two topics, followed by a review of observations of the azimuthal-mean radial TC vortex structure.

1.2. Vortex Resiliency to Vertical Wind Shear

The importance of moist convective processes in the intensification and maintenance of axisymmetric TCs is now well known and reasonably understood (e.g., Ooyama 1969; Rotunno and Emanuel 1987). Recent theoretical studies, however, have attempted to elucidate the role that dry adiabatic dynamics play in the non-axisymmetric vortex response to the impinging vertical shear. Initially barotropic ideal vortices were

considered in these studies to simply explain the effect of shear on just the cyclonic portion of a TC vortex (Reasor et al. 2004). Jones (1995; hereafter J) showed that an initially tilted vortex tends to resist vertical shear by cyclonically precessing upshear and tilting over slowly in comparison to the timescale of the shear advection. The fact that some of their initial vortices eventually succumbed to weak vertical shear may be misinterpreted that moist convective processes are essential for maintaining upright TCs in realistic environments possessing vertical shear. Although a cyclonic precession also occurred in a nearly identical dry adiabatic numerical simulation by Reasor et al. (2004), their vortices remained vertically coupled in a nearly upright configuration, in contrast to some of the vortices employed by Jones (1995). The results of Reasor et al. (2004) suggest that even without moist processes TC-like vortices are more resilient to vertical shear, as suggested in an earlier study by Wang and Holland (1996). The source of the discrepancy between the vortex simulations in these two studies was the initial specification of the azimuthal-mean radial structure of the *idealized* barotropic vortex. Why, then, is the radial structure so important in supporting vortex resiliency to vertical shear?

Recent theoretical studies explain, from different perspectives, the evolution of an initially tilted or vertically sheared geophysical vortex using vortex Rossby wave (VRW) theory (Reasor and Montgomery 2001; Schecter et al. 2002; Reasor et al. 2004; Schecter and Montgomery 2003, 2004). In the linear VRW formalism, the precession of the vortex and its alignment can be represented as the propagation and amplitude-decay of VRW disturbances that propagate on the radial potential-vorticity-gradient wave-guide of the azimuthal-mean vortex. Depending on the mean vortex Rossby number and the ratio of the horizontal scale of the vortex to the far-field internal Rossby deformation radius, the tilt decay for TC-like vortices occurs either via outward propagating sheared VRW disturbances or resonance damping of a VRW quasi-mode (see Reasor et al. 2004 for further details). The sheared route of tilt decay is analogous to the familiar Thomson/Orr decay mechanism for sheared disturbances (Thomson 1887, Orr 1907, Montgomery and Kallenbach 1997, McWilliams et al. 2003). The resonant-damping route of tilt decay (Briggs et al. 1970) can be demonstrated analytically for the particular case of a Rankine-with-skirt (RWS) vortex (Fig. 1.1) in which the non-zero "skirt" of vorticity outside the core represents a small departure from a Rankine vortex in

the sense that the peripheral mean circulation is small compared to that of the vortex core (Schecter et al. 2002, Schecter and Montgomery 2003). Here the tilt decay rate is proportional to the *negative* radial gradient of Rossby-Ertel Potential Vorticity (PV) (Hoskins et al. 1985) at a *critical radius* beyond the radius of maximum azimuthal-mean tangential wind (RMW), where the precession frequency of the vortex tilt matches the rotation rate of the mean azimuthal flow.

Linear VRW theory includes the possibility of a growing tilt asymmetry. If the radial PV gradient is positive at the critical radius then the VRW representing the tilt asymmetry will grow exponentially in time, with an e-folding time scale that is comparable to the advective time scale of the vortex core (Schecter et al. 2002; Reasor et al. 2004; Schecter and Montgomery 2003, 2004), Gent and McWilliams 1986). Reasor et al. (2004) demonstrated that this indeed occurred in the Jones (1995) simulation. The positive radial PV gradient at the critical radius and consequent "tilt instability", originating from the transition of cyclonic to anticyclonic relative vorticity not far beyond the RMW, is characteristic of a class of idealized vortex profiles based upon Smith (1990; hereafter termed 'J vortices', see Fig. 1.1. Gent and McWilliams (1986) studied a related class

of geostrophic vortices). In contrast, the tilted vortices in Reasor et al. (2004) realigned because the family of vortices considered there, including the Gaussian PV distribution (Fig.1.1), possessed monotonically decreasing radial distributions of positive PV and sufficiently *negative* radial PV gradients at the critical radius.

Clearly, the stable or unstable vortex response to vertical wind shear in these idealized (adiabatic) TC models is critically dependent on its radial structure. When moist processes are included, however, the sheared TC problem is more complicated. Nevertheless, Reasor et al. (2004) argues (their Sec. 1) that the tilt dynamics is still controlled in a first approximation by dry adiabatic dynamics. When a hurricane-strength barotropic vortex with a realistic Rossby deformation radius is subject to a simple tilt perturbation, the critical radius is found to lie between one and four RMW distances (Schecter and Montgomery 2003; Reasor et al. 2004). Guided by now well-accepted reasoning that moist processes in the eyewall region give rise to a reduced effective static stability (e.g., Emanuel et al. 1987, Montgomery and Farrell 1992, Shapiro and Montgomery 1993), the critical radius should reside radially inward from its dry estimate (Reasor et al. 2000, Sec. 5). Since precise critical radii for

various tilt perturbations depends to some extent on the radial structure of the initial vortex and also on the moist convective processes whose precise impact has not been worked out, a conservative approach is adopted here by assuming that the moist critical radius lies between 1-3 RMW distances for the vertically-averaged azimuthal-mean vortex.

The foregoing discussion naturally raises important questions for the TC problem: In theoretical studies, how realistic are the idealized vortex profiles used in representing the radial (PV) structure of TCs? What is the true radial structure of TCs?

1.3. Vortex Structure and Intensification

The lack of a generally accepted definition of rapid intensification explains part of our lack of understanding of this phenomenon. Brand (1973) arbitrarily defined rapid intensification as a minimum 50 knot increase in the maximum sustained wind speed in a 24-hour period and noted the rarity of this phenomenon for western North Pacific typhoons. Holliday and Thompson (1979) classified rapidly intensifying typhoons as those that experienced central pressure falls of at least 42 mb in 24 hours. This definition was statistically based and represented the upper 25% of *maximum* 24-hour central pressure falls in 305 storms. A less stringent

definition of rapid intensification has been developed for the Atlantic basin in a recent statistical study by Kaplan and DeMaria (2003). They determined a maximum wind speed increase of at least 30 knots (15.4 m/s) in 24-hours, defined by the 95th percentile of all (overlapping) over-water 24-hour intensity changes from the best-track data record during 1989-2000. These somewhat arbirtrary definitions based only on statistics, however, do not reveal much physical understanding of rapid intensification.

A definition of rapid intensification based on physical processes is ultimately desired for the understanding of this phenomenon. The inability of statistical and dynamical models to anticipate extreme changes in intensity, discussed previously, is a testament to our fundamental lack of understanding. The physical processes that are considered to influence tropical cyclone intensification in general are internal dynamics, large-scale environmental interactions, and ocean-atmosphere interactions. Most work that concerns the specific causes of rapid intensification events, however, has focused on the latter two areas. For instance, recent speculation of the causes of hurricane Opal's (1995) explosive intensification includes a jet-trough-hurricane interaction

(Bosart 2000) and the interaction with an oceanic warm core eddy (Black and Shay 1998, Hong et al. 2000, Shay et al. 2000).

The understanding of the rapid intensification phenomenon may be further improved by investigating its relationship to the structure of TCs. This approach may yield clues to the responsible physical mechanisms and perhaps reveal precursors that may indicate future rapid intensification. As discussed in the previous section, in which the VRW theory reveals that the radial TC structure may be essential for the vortex integrity, it is worth investigating whether the radial structure may itself influence future intensification of the storm in question.

Perhaps the most widely accepted theory concerning the evolution of the symmetric swirling wind structure is the *Convective Ring Model of Intensification*, which states that a local tangential wind maximum, associated with an annular ring of intense convection that encircles the cyclone center, contracts inward as the cyclone intensifies. This theory was proposed as a result of an aircraft observation/model comparison study by Willoughby et al. (1982) in their attempt to explain the behavior of inner and outer eyewalls in very intense cyclones. Willoughby's (1990a) similar study generalized the theory to explain all intensifying storms.

With the aid of multiple high-resolution radial leg penetrations into Atlantic storms, they estimated the short time-scale evolution (several hours) of the symmetric structure by calculating the tangential wind tendency during a particular flight mission. Figure 1.2 shows an example of a contracting tangential wind maximum and the associated convective rings during the intensification of Hurricane Alicia (1983).

This phenomenon can be explained in terms of Willoughby (1979) and Shapiro and Willoughby's (1982) application of the Eliassen (1951) symmetric balanced vortex theory to tropical cyclones. In essence, the primary circulation of a symmetric vortex in hydrostatic and gradient wind balance will gradually evolve in response to the diagnosed transverse secondary circulation that is forced by imposed point sources of heat and momentum. By specifying a heat source and vortex structure similar to that observed in Hurricane Allen (1980), excellent agreement is obtained between model (Fig. 1.4) and observed (Fig. 1.3) tendencies of tangential wind and geopotential height. Greater height falls are induced inside the RMW where the intense heat source is located, as opposed to lesser height falls outside the RMW where the heating is more diffuse. The large radial gradient in height tendency corresponds to a peak in the tangential wind

tendency (via gradient wind balance) at this location inside the RMW. This results in an apparent contraction of the tangential wind maximum and a more sharply peaked tangential wind profile. The tangential wind tendencies can also be explained in terms of intense momentum advection by the diagnosed secondary circulation. Willoughby (1990a) speculated that the convective ring model accounted for the intensification of most major hurricanes.

The Shapiro and Willoughby model also explains the more complicated behavior of concentric eyewalls, in which the remote heat source associated with the outer convective ring induces subsidence and lower tropospheric outflow near the vortex center, resulting in negative tangential wind tendencies near the inner eyewall and the concomitant ceasing, or at least slowing, of intensification. The resultant tangential wind profile becomes relatively broad and flat with the decay of the inner wind maximum. The eyewall replacement cycle may be completed, (unless inhibiting influences such as landfall occur first), in which the outer eyewall contracts and eventually supplants the inner eyewall as the vortex re-intensifies.

Willoughby (1990a) concluded, after examining the vortex behavior of many TCs, that: 1) the most rapidly intensifying storms in his study were characterized by sharply peaked wind profiles associated with single, vigorous axisymmetric convective rings and associated sharply peaked wind 2) slowly intensifying storms are characterized by rings of weak, cellular convection and relatively flat wind profiles, and 3) non-developing tropical storms also possessed flat wind profiles along with asymmetric convection that couldn't support sustained intensification.

The observed shape of the tangential wind profile for the TCs in Willoughby's (1990a) study was clearly a consequence of the rate of intensification. For example, the most rapidly intensifying TCs characterized by sharply peaked profiles resulted from the contracting and increasing tangential wind maxima. Although theory (Shapiro and Willoughby 1982) does explain to some degree the TC vortex evolution during intensification (in response to heat sources), the importance of the initial vortex structure on the future intensification has not been revealed. The central question here concerns how the observed initial vortex structure may influence the future intensification and structural evolution. In other words, is the radial profile of the tangential wind *prior* to rapid

intensification different in comparison to slower developing storms of similar intensity? Is there a characteristic feature of the azimuthal-mean radial vortex structure that indicates rapid intensification will occur?

1.4. Review of Tropical Cyclone Radial Structure

The questions raised in the preceding two sections regarding the TC vortex resiliency and intensification necessitate a review of the azimuthal-mean radial structure. The first part concerns recent observations of radial PV structure and is primarily directed at the vortex resiliency topic. The second part is a more general historical review of the radial structure of the tangential wind and naturally applies to both vortex resiliency and intensification.

1.4.1. *Potential Vorticity*

For the particular theoretical discussion concerning the vortex resiliency of *initially barotropic* TC-like vortices in a PV framework, to the observation of the full three-dimensional kinematic and thermodynamic structure of a TC would be ideal for the purpose of estimating its vertically-averaged and azimuthal-mean radial PV structure. In the most comprehensive analyses of a single TC performed to date, Shapiro and Franklin (1995) calculated PV for the vortex core and environment of

hurricane Gloria (1985) from a multitude of data sources, such as Omega dropwindsondes (ODWs), Doppler radar and various synoptic datasets. The radial-height cross-section of Gloria's azimuthal-mean PV structure (from Shapiro and Franklin 1995) and tangential wind (from Franklin et al. 1993) is shown in Figure 1.5. Monotonically decreasing positive PV (Fig. 1.5a) extends throughout the depth of the troposphere and radially outward to at least 500 km from the center, except in the small core region at the highest levels and inward of the secondary PV maxima located at mid-levels near 100 km radius. Since the tangential wind maximum throughout the tropospheric depth is located near the 20 km radii (Fig. 1.5b), the critical radius is likely to reside somewhere between 20 – 60 km (1-3 RMW distances), a region of negative PV gradient for the vertically-averaged vortex. On the basis of the discussion in section 1.2, Hurricane Gloria would thus be expected to remain resilient to vertical shear in weak to moderately sheared environments.

Unfortunately, the kinematic and thermodynamic data necessary for the calculation of PV throughout the tropospheric depth is not widely available, Gloria (1985) being the notable exception. There exists, however, a wealth of knowledge of TC structure based on observations of the

swirling circulation, prior to the popularization of PV dynamics in TC studies.

1.4.2. *Tangential Wind*

Historically, the primary circulation has been a particular focus of many TC structure studies. Depperman (1947) was apparently the first to apply the Rankine vortex to approximate TC structure. The Rankine vortex is characterized by solid body rotation (uniform angular velocity) within the RMW and conserved relative angular momentum outside, i.e., $Vr = const.$ where V is the tangential velocity component (e.g., Batchelor, 1967). The frictional loss of cyclonic relative angular momentum of inward spiraling boundary layer air familiar to TCs, however, required a modification to the Rankine vortex, $Vr^{\alpha} = const.$ where $0 < \alpha < 1$ (Hughes 1952; Riehl 1954). Riehl (1963), and more recently Pearce (1992), have argued theoretically that with the typical specification of boundary layer frictional drag, $F \sim V^2$, the tangential wind speed in steady-state mature hurricanes must decrease with radial distance as $V \sim r^{-1/2}$. Pearce (1992) elegantly demonstrated this by showing that in angular momentum coordinates (Thorpe 1985) the radial gradient of the frictional torque, $\partial(rF)/\partial r$, for a steady-state axisymmetric vortex in gradient wind balance

must vanish in the convective inflow region, since the other terms (heating, vertical advection) in the PV tendency equation are negligibly small there.

The nature of the inflow layer underneath a TC supports the many observational studies showing that the tangential winds in TCs approximately decrease similar to a modified Rankine vortex, although the decay exponent has been shown to vary. Many studies of mature storms were found to have decay exponent values for α between 0.5 and 0.7 (Hughes 1952; Malkus and Riehl 1960; Riehl 1963; Miller 1967; Sheets 1980; Anthes 1982; Franklin et al. 1993). Shapiro and Montgomery (1993), however, indicate that smaller values ($\alpha < 0.5$) are evident in the storms studied by Riehl (1963) and Willoughby (1990a), which were at weaker stages of intensity. This apparent variability was confirmed in the multi-storm statistical studies of Gray and Shea (1973) and Samsury and Zipser (1995), where mean values found for α (0.5 and 0.4, respectively) were close to the expected theoretical value, but with relatively large standard deviations (0.3 and 0.2, respectively). It is believed that the stage of TC lifecycle accounts for much of the variability in the outer profile shape, as demonstrated by Weatherford (1989). Many of the studies discussed, however, do not clearly specify the radial region used for the estimation of

the modified Rankine decay exponent. Indeed, Petrova (1995) demonstrated that α increased for radial intervals located at increased distances from the center of western North Pacific typhoons, with values approaching unity in the outer core region. This is in agreement with the large values evident at large radii in the composite Atlantic storm of Merrill (1984), as pointed out by Shapiro and Montgomery (1993).

The preceding discussion was based primarily on results from observational studies of low-level and mid-level tangential winds obtained from flight missions into Atlantic, Eastern Pacific and western North Pacific TCs. Though scarce, observations at upper levels have revealed a larger modified Rankine tangential decay exponent than at low and middle levels. The tangential wind structure of hurricane Gloria (Fig. 1.5a) clearly illustrates this, in agreement with the results of Shea and Gray (1973) and Frank (1977, his Fig. 9). However, the tangential wind decay for this case is still less than that of a pure Rankine vortex in the near-core region and, more importantly, the mean tropospheric layer vortex beyond the RMW likely possesses the approximate radial structure of a modified Rankine vortex.

1.5. Objectives of Thesis

In an ideal situation the radial PV structure of real TCs would be compared with analytic profiles. As already discussed, this is not currently practical or possible for a large number of storms. However, relative vorticity may serve as a proxy for PV at single vertical levels, as in the recent flight-level observational study of the hurricane eye and eye-wall region performed by Kossin and Eastin (2001). Following this approach, the aforementioned science questions in Section 1.2 are addressed by comparing flight-level observations of tangential wind and relative vorticity, which are more widely available, with their equivalent idealized radial profiles.

Prior studies indicate that the modified Rankine vortex is a more realistic depiction of the tangential wind structure than pure Rankine vortices. The question remains as to how realistic are other ideal vortex profiles used in theoretical studies. In particular, how realistic are the family of vortices used by Jones (1995) and Reasor et al. (2004) (see Fig. 1.1) that give contrasting results in the vortex resiliency problem? How realistic is the larger tangential wind decrease of the J vortex in this region? Is the location of *anticyclonic* relative vorticity too close to the

RMW? These particular vortex features, and the associated positive radial vorticity gradient, clearly differentiate the J vortex from the other idealizations shown.

To our knowledge the current re-examination of the radial structure of tangential wind and relative vorticity for TCs of all intensities and scales is the most comprehensive ever undertaken using flight-level observations. For reasons discussed above, the specific focus is upon the near-core region between 1-3 RMW distances in which the modified Rankine vortex is applied in a consistent manner to roughly estimate the radial TC structure. This particular vortex region has not been specifically emphasized in prior studies of the primary circulation. In one respect, the broadness of the tangential wind structure is confirmed, as suggested in the earlier studies discussed. What distinguishes this study, however, is the additional emphasis on the associated skirt of cyclonic relative vorticity observed in all TCs in the near-core region beyond the RMW. The current evidence of Reasor et al. (2004) and Schecter and Montgomery (2003, 2004) suggest that this region is of critical importance in supporting the resiliency of TCs subject to hostile vertically sheared environments. These structural characteristics intrinsic to all TCs, are shown to be

deficient in some analytic vortex profiles commonly used in theoretical studies of TC evolution. This study will thus, in effect, establish some "ground truth" for the idealization of vortex structure.

Having established the basic TC structure necessary for vortex resiliency, a further understanding of how the primary circulation may influence the intensification is attempted, despite the limited current state of our theoretical understanding. Specifically, the primary focus concerns whether the tangential wind structure of rapidly intensifying TCs is distinguished from slowly or moderately intensifying systems. Th e findings presented in this thesis reveal that no unique structural characteristics of the azimuthal-mean tangential wind can predict with certainty that rapid intensification will commence or continue. However, there is some evidence that necessary, but not sufficient, conditions may exist in the tangential wind structure prior to the largest intensification periods. The additional requirements for rapid intensification, in terms of the role of thermodynamics, asymmetric structures and overall vortex organization is speculated and discussed.

CHAPTER 2. DATA

Two data sets are used in this study of Atlantic and Eastern Pacific tropical cyclones. The National Oceanic and Atmospheric Administration (NOAA) Hurricane Research Division (HRD) archive of aircraft reconnaissance data (1977-2001) is well suited to study the radial structure and is the primary data set. The National Hurricane Center's (NHC) "best track" data set additionally provides a consistent measure of the TC intensity.

2.1. Flight-level Aircraft Reconnaissance Data

The primary data were extracted from the NOAA/HRD archive comprising flight-level aircraft observations of Atlantic and Eastern Pacific tropical cyclones between 1977 and 2001. During flight missions, data are acquired at, or near, a specified standard pressure level (900, 850, 700, 600, 500 and 400 mb) along multiple radial "legs" at different azimuths with respect to the TC center, directed either inwards or outwards. Measurements of geopotential height, wind velocity, temperature and its dewpoint, and the liquid water content are collected

from NOAA WP-3D and United States Air Force (USAF) WC-130 aircraft at frequencies of 0.1 and 1.0 Hz, respectively.

The data processing for the HRD archive requires two key procedures. First, the original raw data is recomputed in a cylindrical-polar coordinate system moving with the TC center, enabling the decomposition of the wind velocity into radial, tangential and vertical components. The required storm center location is estimated for each radial pass through the center using the algorithm of Willoughby and Chelmow (1982). Second, the data are smoothed and interpolated to a 300-point radial grid with nominal 0.5 km grid spacing[1] using a Bartlett filter. Specifically, the data are weighted and placed into overlapping bins of 2.0 km width and averaged, the weighting factor decreasing linearly decreasing from unity at the bin center (grid point location) to zero at the boundaries. Further detailed discussion of aircraft instrumentation and data processing can be found in Jorgensen (1984), Willoughby et al. (1982) and Samsury and Zipser (1995).

---

[1] There exist several flight missions where the maximum radial extent of the data is either 300 km (Arthur 1984, Gloria 1985) or 75 km (Emily 1987). Since the number of data points in the radial array is fixed (300) in the HRD database, the nominal 0.5 km grid spacing is effectively doubled (1.0 km) or halved (0.25 km).

The resulting HRD database (1977-2001), organized by storm and flight mission, is comprised of radial arrays of data representing the kinematic and thermodynamic variables from the storm center outward to a maximum 150 km radial extent at 0.5 km intervals. A total of 5124 radial legs of data were obtained from 644 missions into 72 storms during this period. The vast majority of flight missions occur between 900 and 600 mb, with the 700 and 850 mb levels sampled most often. Relatively few aircraft penetrate TCs at 500 mb and only several flight missions at 400 mb were performed. Of the meteorological variables available in the HRD archive, only the tangential component of the wind velocity is needed for this study. The raw horizontal wind measurements are accurate to within 1.0 and 2.0 m s^{-1} for the NOAA WP-3D and USAF WC-130 aircraft, respectively (OFCM 1993; Kossin and Eastin 2001). This degree of accuracy is due to the modern inertial navigation (INE) system, greatly improved over the Doppler aircraft navigation used prior to the mid-1970s (Willoughby 1990b). However, more error is likely to be introduced into the transformed wind components in the HRD database, due to the uncertainty in the storm center location (Samsury and Zipser 1995).

2.2. NHC Best Track Data

The NHC best track database is comprised of 6-hourly estimates of tropical cyclone position and intensity for North Atlantic and Eastern Pacific storms dating back to 1851 and 1949, respectively. NHC forecasters and researchers determine the final best track data by re-analyzing all of the available observations from aircraft, satellite, radar and synoptic data platforms in the hurricane post-season. Two values of intensity are given, the maximum sustained wind speed (1-minute average) at the surface (10 m height) and the central sea-level pressure of the storm. Both will be considered to represent the intensity and intensity change.

2.3. Extended Best Track Data

An extended version of the NHC best track dataset (1988-2003) additionally includes NHC operational estimates of the radius of maximum wind, eye diameter, pressure of the outermost closed isobar (POCI), radius of the outermost closed isobar (ROCI), and radii of 34, 50, 64 knot winds speeds to the NE, SE, SW, NW of the storm center. This data set was originally funded by the Risk Prediction Initiative and is now updated by NESDIS/ORA for satellite algorithms used in TC analyses and is maintained by Mark DeMaria from CIRA/CSU. Since no attempt has

been made for quality control, the storm size estimates and eye-size of interest here are not intended for serious analysis and referred to in casual discussion and speculation.

CHAPTER 3. METHODOLOGY

3.1. Calculation of Azimuthal-mean Radial Vortex Profiles

The estimation of the azimuthal-mean radial structure of tangential wind and relative vorticity is desirable for the comparison with idealized vortex profiles that represent the axisymmetric TC structure in theoretical studies. This procedure has the added practical advantage of reducing the data set to one radial profile per flight mission, in which the individual radial legs of data possess similar structure.

3.1.1. *Tangential Wind*

In general, the degree of circular symmetry in the tangential wind field of hurricanes increases with intensity (Croxford and Barnes 2002). Pre-hurricane structure can be relatively disorganized and may exhibit less azimuthal symmetry than hurricanes (e. g. Stossmeister and Barnes 1992); the tangential wind may vary significantly in the different quadrants of the storm. The majority of TCs in this study, however, possess sufficient structural coherence in the tangential wind field for a distinct maximum to be evident in the azimuthal-mean component. This is important for making comparisons with idealized wind distributions.

The accurate estimation for a radial profile of an azimuthal-mean quantity necessitates an approximately even azimuthal distribution of flight legs among the storm quadrants. Fortunately, most flight missions consist of one or more complete "figure-four" patterns, in which data is obtained along four equally spaced radial legs, most often in the N-S-E-W or NW-SE-NE-SW directions (8 radial legs on average). A minimum of four radial legs, one from each storm quadrant is thus required. Another consideration is the accurate estimation of the azimuthal-mean structure for a potentially rapidly evolving TC sampled over the finite time period of a flight mission, which varies (six-hour average) among different storms and flight missions. Willoughby et al. (1982) and Willoughby (1990a,b) applied least-squares methods to the time-dependent data in order to calculate tendencies during a flight mission, enabling the estimation of the azimuthal-mean tangential wind at any time during the flight period. For our study, however, a "snapshot" of the azimuthal-mean tangential wind representing the midpoint of the flight mission is sufficient. A good approximation is simply the arithmetic average over the number of available radial legs N at each radius r_i,

$$\overline{V}_i = \frac{1}{N}\sum_{j=1}^{N} V(r_i, \lambda_j) \qquad (1)$$

where the subscripts i, j denote the radial and azimuthal bin locations, respectively.

An accurate and complete depiction of the azimuthal-mean radial profile, however, is not always possible using all of the available data from a given flight mission. The prohibition from flying over land for an approaching storm limits the radial extent of the flight legs in the storm quadrant nearest landfall (Willoughby 1990a). Cases with insufficient data in one or more quadrants were not considered for this study. Another consideration is the regions of missing data that are sometimes present in the individual radial legs, resulting from instrumentation failures and tape changes (Willoughby et al. 1982). Inclusion of the radial legs in the averaging process can result in discontinuities in the calculated azimuthal-mean radial profile. Small gaps ($\leq$ 10 km) were filled by linear interpolation or removed in the event that the primary wind maximum was located there. Radial legs with large regions of missing data (> 10 km) were selectively removed. For example, two short radial legs of data (located north of center) obtained on a flight mission into hurricane Andrew (Fig. 3.1) were removed from the averaging process since the radial extent of data was limited both within and outside the RMW. In this

particular case, the procedure also improved the symmetry in the azimuthal distribution of the remaining radial legs.

To summarize, the estimation of the azimuthal-mean tangential wind profile was performed by choosing the optimal subset of radial legs available during a given flight mission for azimuthal-averaging that maximizes the radial extent within and outside the RMW, while retaining a reasonably balanced degree of symmetry in the azimuthal distribution of the radial legs. The resulting azimuthal-mean profile was smoothed using a 5 km (9 points) Bartlett filter, which has the advantage of preserving the locations of peak values.

3.1.2. *Relative Vertical Vorticity*

The radial profiles of azimuthal-mean relative vertical vorticity are most easily estimated from the smoothed azimuthal-mean tangential wind component of relative vorticity $\bar{\zeta}$ is related to the symmetric tangential wind $\bar{V}$ by the equation $\bar{\zeta}(r) = \bar{V} / r + d\bar{V} / dr$. The shear term in the relative vorticity is approximated by centered differencing, resulting in $\bar{\zeta}(r_i) = \bar{V}(r_i) / r_i + (\bar{V}_{i+1} - \bar{V}_{i-1}) / (r_{i+1} - r_{i-1})$, where subscripts denote the radial grid location.

3.2. Non-dimensional Composite Radial Vortex Profiles

The estimation of the *mean* tangential wind field from radial profiles of different storms has been performed in past studies in which two composite methods have been used. One method involves the averaging of tangential wind observations at each radius, as measured from the storm center. This method was sufficient for the intentions of Hughes (1952) and Weatherford (1989), who composited radial profiles to large distances well beyond the RMW, utilizing outer vortex observations of western North Pacific typhoons. This method, however, is not useful for resolving common tangential wind features inside the RMW from storms of widely varying radial scale. This problem was overcome in Shea and Gray (1973), and more recently in Samsury and Zipser (1995), by shifting the radial data to a common RMW before averaging. This method of averaging with respect to radial distance from the RMW is considered more relevant for understanding inner core dynamics of TCs, by separating profile features inside and outside of the RMW (Shea and Gray, 1973).

A novel composite method is introduced here for the purpose of obtaining the mean underlying radial structure of a group of radial vortex

profiles of varying intensity and radial scale. Prior to averaging, the individual azimuthal-mean tangential wind profiles are appropriately scaled by dividing by the maximum value (V_{max}), and the radius by the RMW, so that each profile possesses a unit maximum located at unit radius. In other words, a non-dimensional composite is obtained by normalizing the individual tangential wind profiles, then averaging with respect to a non-dimensional radius. By removing the scales for the azimuthal mean tangential velocity (V_{max}) and its radius (RMW), the characteristic underlying profile shape is preserved. The non-dimensional composite method, however, has an additional complication that is not present in the other two methods discussed. The radial scaling in this method results in a different non-dimensional radial grid spacing for each case belonging to a group of profiles to be averaged. This difficulty is overcome by choosing the non-dimensional radial array with the *smallest* grid spacing, i.e., the profile(s) with the *largest* RMW, to be the common radial grid for averaging. The data from each normalized tangential wind profile, with radial grid spacing at least as large as the common grid, is simply linearly interpolated to this common radial grid and then averaged. Hence, the radial resolution is not compromised. The non-dimensional

radial extent (in RMW units) of the composite profile will of course be limited by the case(s) with the largest RMW.

The relative vorticity is normalized to the value at the RMW (V_{max}/RMW), consistent with the scaling used to non-dimensionalize the tangential wind. This method is well suited for this study because it facilitates comparison with idealized vortex profiles, which are often expressed in non-dimensional form (Appendix A).

Figures 3.2 and 3.3 illustrate and compare the three methods discussed here for the tangential wind and relative vorticity, respectively. Clearly, the first method is undesirable since the resultant composite tangential wind profile is broad and flat in shape, unlike any of the individual profiles. Important features of the profiles are not resolved (Fig. 3.2a, 3.3a). The second method is an improvement since the wind maximum is preserved. However, each profile possesses a different radial scale and much variability remains (Fig. 3.2b, 3.3b). Our method results in a composite profile that is representative of the underlying characteristic shape. Note the uniformity in the individual profile shapes (Fig. 3.2c, 3.3c).

3.3. Intensity and Intensity Change Estimates

For this study, an estimate of intensity associated with the radial structure is needed for the purpose of TC classification. The flight-level maximum azimuthal-mean tangential velocity (V_{max}), obtained from the estimated radial profiles and needed for normalization (discussed in previous section), is a good measure of the vortex intensity. Alternatively, the maximum sustained surface wind speed (V_m) and central pressure (P_c), which may also represent the intensity, can be estimated by interpolating the NHC best-track data to the midpoint of each flight mission.

In comparing the two wind speed estimates, Willoughby and Rahn (2004) speculate that the reduction of the maximum flight-level wind speed by azimuthal-averaging is approximately equal to the reduction of the wind speed to the surface. A scatter diagram of V_{max} and V_m (Fig. 3.4), however, reveals that the azimuthally-averaged flight-level tangential wind maximum actually underestimates the surface wind maximum by approximately 5 ms^{-1}. The stratification by flight level in Fig. 3.4 reflects the common practice of higher altitude aircraft reconnaissance missions as storm intensity increases (for safety reasons). Note that except for the very weakest intensities, there is no apparent systematic difference in the V_{max}/

V_m relationship for different flight levels. In a mean sense, it is thus reasonable to mix flight levels when analyzing a large numbers of cases. Therefore, V_{max} will be the primary measure of intensity in the statistical composites in Chapter 4 and the investigation of the relationship between tangential wind profile parameters and the intensification rate in Chapter 5. For the purpose of comparing a small number of cases, when TC intensity classification is important, the best-track estimate is used.

An estimate of intensity change from the flight-level data, though desirable, is not guaranteed to be available. Although the majority of flight missions are performed at 12-hour intervals, there often may not be any flight-level data available into the future. The change in flight level as a storm is intensifying could also lead to an inaccurate estimate of the intensity change. For a consistent estimate of the future intensification the NHC best-track data is employed to calculate a 24-hour change in maximum wind speed (ΔV_{24}) and minimum central pressure (ΔP_{24}) by simply taking the difference between the interpolated values at the midpoint of the flight mission and at a specified time in the future.

For this study of Atlantic and eastern North Pacific TCs, the Kaplan and DeMaria (2003) criterion ($\Delta V_{24} > 15.4$ ms^{-1}, or 30 kts) will be used to

distinguish the rapidly intensifying TCs. The use of this particular definition will be justified in Chapter 5.

CHAPTER 4. VORTEX RESILIENCY

4.1. Parameter Specification of Tangential Wind Profile

The requirements for calculating the azimuthal-mean radial TC structure (Section 3.2) yield a subset comprising 525 pairs of observed radial profiles of tangential wind and relative vorticity, each pair representing a single flight mission. The distribution of the observations in terms of the fundamental scales, RMW and V_{max}, is depicted in Fig. 4.1. The range in V_{max} spans all intensity classifications from tropical depressions to Category 5 hurricanes. There is essentially no statistical relationship between the RMW and V_{max} except for the most intense storms, where V_{max} tends to be located close to the TC center, consistent with the results of Shea and Gray (1973). The range in RMW is large, from 9 to 178 km. Note, however, that the 150 km radial constraint may preclude the observation of the true V_{max} in some cases.

For this study, the primary interest is the vortex structure between 1 – 3 RMW distances, due to the location of the critical radius. This radial range, however, can only be investigated for the cases where the RMW is at most within 50 km of the cyclone center. Fortunately, the greatest density of observations is located here (Fig. 4.1) and comprises 60% of the

available mean vortex profile pairs. The 3 RMW data requisite further limits the sample to 255 cases, since not all azimuthal-mean profiles extend to 150 km. For the remaining cases with RMW beyond 50 km, the vortex profile is observed to less than three RMW distances from the TC center, as a consequence of the 150 km radial constraint.

To characterize the vortex structure beyond the RMW, the modified Rankine decay exponent α is calculated for all azimuthal-mean tangential wind profiles. This is one way to further specify, in addition to the RMW and V_{max}, the azimuthal-mean radial structure. Values of α were estimated for individual cases by using the following relationship derived from (A1):

$$\frac{V_1}{V_3} = \left(\frac{r_3}{r_1}\right)^{\alpha} \tag{2}$$

where the azimuthal-mean tangential wind speeds are specified at one and three RMW distances from the TC center. This simple approach was used in order to approximately represent the tangential wind decay in a relatively limited radial range (1-3 RMWs); rigorous curve fitting (e.g., least-squares method) was believed to be unnecessary for this study.

The relationships between the RMW and V_{max} with α are depicted in the scatter diagrams in Fig. 4.2. For the subset of cases with RMW within

50 km, the lack of correlation between RMW and α is obvious (Fig. 4.2a), suggesting that the tangential wind decay is independent of radius. In contrast, a clear relationship exists between V_{max} and α (Fig. 4.2b). In general, as the TC intensity increases, the RMW becomes smaller and the tangential wind profile becomes more sharply peaked (Willoughby et al. 1982, Willoughby 1990a). This is particular true for rapid intensification scenarios, which is discussed in Chapter 5.

4.2. Observed Versus Idealized Vortex Profiles

To simplify the problem, the pairs of mean vortex profiles (tangential wind and relative vorticity) are grouped into three types based on the maximum azimuthal-mean tangential velocity V_{max} (Table 4.1). The ranges in V_{max} that define the three categories are somewhat arbitrary, and approximately represent the common characterization of pre-hurricane, minimal hurricane and major hurricane categories, which are commonly defined in terms of the ground-relative maximum surface wind speed.

In order to efficiently compare the large number of observed vortex profiles to the idealizations, non-dimensional composite profiles of tangential wind and relative vorticity are constructed for each TC class, as

discussed in Chapter 3.2. The resulting pair of mean vortex profiles for each TC class is then compared with Rankine, Gaussian and J idealized vortex profiles (refer to Fig. 1.1 for comparison with RWS vortex) in addition to the best-fit modified Rankine vortex. The variability in each class and for the total sample (RMW $\leq$ 50 km) is summarized in Table 4.1. In addition, to completely demonstrate the full range of vortex behavior beyond the RMW, three individual storms (one from each TC class) characterizing the mean and two opposite extremes are discussed.

4.2.1. *Pre-hurricane storms*

Pre-hurricane structure has been previously characterized as possessing large RMWs with broadly shaped wind profiles (e.g., Willoughby 1990a). Many of the tangential wind profiles of strong tropical storms in this study, however, exhibit sharply peaked wind maxima located relatively close to the storm center (within 50 km), a characteristic typically ascribed to more developed cyclones. A composite radial profile of azimuthal-mean tangential wind and relative vorticity from all 75 pre-hurricane cases are shown in Fig. 4.3 and compared with the idealized vortex profiles.

Within and near the RMW, the mean pre-hurricane tangential wind profile shape is broader than the sharply peaked Rankine vortex profile but not quite as broad as a Gaussian vortex. This corresponds to the larger than Gaussian, yet finite, gradient of relative vorticity across the RMW. Just beyond the RMW, the rate of tangential wind decrease is much less than the rapid decay of a pure Rankine vortex but is initially greater than Gaussian and J vortices. Although the corresponding relative vorticity is slightly lower than Gaussian values just beyond the RMW, it is still appreciably non-negative, in contrast to the characteristic zero vorticity of a Rankine vortex.

Most pertinent for this study, however, is the region farther outward from the wind maximum between roughly 1.5 and 3 RMW distances from the center. Here, the mean pre-hurricane tangential wind, similar to the equivalent modified Rankine vortex (α=0.30), decreases more slowly with distance than the Gaussian vortex and therefore slower than all other idealizations. This naturally corresponds to the slower monotonic decrease in relative vorticity, and thus overall greater values of relative vorticity of the mean pre-hurricane vortex in this region. This is in sharp contrast to the rest of the ideal vortices, whose exaggerated

tangential wind decrease results in negligible (Gaussian), zero (Rankine) or even negative (J vortex) relative vorticity. It is quite clear that these idealized vortices are highly unrealistic in representing the mean pre-hurricane vortex structure in the near-core region outside of the RMW.

As an example, consider Atlantic tropical storm Fran in its early stage of development on August 30, 1996. Although the tangential wind and relative vorticity profiles (Fig. 4.4) resemble the Gaussian vortex from within and just outside the 24 km RMW, they quickly diverge from all of the idealized vortices beyond approximately 30 km. The tangential wind decreases very slowly to 70-75 km (~3 RMWs) with an approximate decay exponent value of α=0.15. The large-scale trend in relative vorticity, despite the small-scale fluctuations (on the order of 5-10 km), is decidedly monotonic decreasing with significantly larger values than all of the idealized vortices. Comparison of Fran with the equivalent modified Rankine vortex (α=0.15) elucidates the appreciably non-zero negative radial gradient of the underlying relative vorticity. This supports our contention that the broadness of the tangential wind profile and the corresponding significant "skirt" of relative vorticity beyond the RMW

distinguish real pre-hurricane structure from some of the unrealistic idealizations commonly used in studies of TC evolution.

4.2.2. *Minimal Hurricanes*

The majority of the observations fall into this classification. Figure 4.5 shows that the mean minimal hurricane vortex profile is qualitatively similar to the behavior of the mean pre-hurricane storm. The mean tangential wind profile shape within roughly 1.5 RMW is broader than a pure Rankine vortex, yet narrower than the equivalent Gaussian vortex. This is again manifested in the sharper than Gaussian decrease of relative vorticity across the RMW yet slower than the discontinuous jump from constant to zero vorticity characteristic of Rankine vortices. As a consequence, significantly non-zero cyclonic relative vorticity exists outside the RMW. The mean minimal hurricane vortex structure beyond 1.5 RMW distances behaves quite differently than the ideal vortices, as in the pre-hurricane group. The fractional (not actual) decrease of tangential wind with distance is greater for the mean minimal hurricane than the mean pre-hurricane storm, with a slightly larger decay exponent for the equivalent modified Rankine vortex (α=0.35). However, in contrast to the idealized vortices, the comparably slow observed tangential wind and

relative vorticity decrease results in their conspicuous broadness in the vicinity outside the RMW.

Category 2 storm Bonnie on 23 August 1998 is a representative case of the minimal hurricane class and can be considered an average case for the sample considered. The vortex behavior (Fig. 4.6) is very similar to the composite minimal hurricane vortex in all aspects, except that the small-scale fluctuations in the relative vorticity beyond the RMW slightly obscure the monotonically decreasing trend that is more clearly evident in the mean relative vorticity (Fig. 4.6b). The slow underlying monotonic decrease of relative vorticity, which can be represented by the $r^{-(\alpha+1)}$ decay of the equivalent modified Rankine vorticity (α=0.35), ensures appreciably non-zero values of relative vorticity (and radial gradients) out to large radii.

4.2.3. *Major Hurricanes*

This final class of vortex profiles to be discussed represents the most intense storms in this study. Inside the RMW, the composite major hurricane vortex profiles (Fig. 4.7, also see Figs. 3.2, 3.3) appear quite different than that of the pre-hurricane and minimal hurricane classes. This group has much less Gaussian vorticity characteristics in this region

than the other two classes (Fig. 4.3b, 4.5b), which can be clearly seen in the deviation from Gaussian relative vorticity (Fig. 4.7b). The very rapid increase in tangential wind speed, far from the linear increase of a Rankine vortex, results in a relative vorticity maximum between the center and the RMW. The latter arises in association with the strong vortex-tube stretching of vertical vorticity by the convective and mesoscale updrafts within the hurricane eyewall (Schubert et al. 1999). These wind profiles are expected to support combined barotropic-baroclinic (shear) instability and related eyewall mesovortex phenomenology (Schubert et al. 1999; Montgomery et al. 2002). Such interior vorticity redistribution processes typically evolve on a smaller (radial shear) timescale than the tilted vortex response (scale separation) and hence should not significantly alter the tilted vortex predictions using monotonic PV distributions summarized in the introduction. This will be assumed for the remaining discussion.

Outside the RMW, the story is qualitatively the same as for the pre-hurricane and minimal hurricane classes. The mean fractional decrease of tangential wind with radius is much greater than both the mean pre-hurricane and minimal hurricane vortex, as evidenced by the larger decay

exponent of the equivalent modified Rankine vortex (α=0.48). This is in agreement with Croxford and Barnes (2002), who found a greater decrease of tangential wind at large radius for more intense storms. Despite these differences, the faster tangential wind decay of major hurricanes is still relatively slow enough to allow for significant relative vorticity (and radial gradients) in comparison to the idealized vortices in the 1-3 RMW radial region. This is essentially the same vortex behavior that the mean pre-hurricane and minimal hurricane classes exhibited.

The case exhibiting the most extreme tangential wind decrease in the entire data set was from this category of hurricane intensity. During 1854-2053Z on 13 September 1988, hurricane Gilbert (Fig. 4.8) was near its peak intensity of 888 mb with a maximum azimuthal-mean tangential wind speed (V_{max}) of nearly 70 m/s. The large tangential wind decrease beyond the RMW resulted in a decay exponent of α=0.67, according to the best-fit modified Rankine vortex between 1-3 RMW distances. The relative vorticity trend, though only slightly obscured by the smaller scale fluctuations, is monotonically decreasing (Fig. 4.8b). Even in this most extreme case (largest α), however, the important skirt of relative vorticity

beyond the RMW is still significantly greater than for equivalent Rankine, Gaussian and J idealized vortices.

4.3. Summary of Results

The preceding results of the vortex structure for pre-hurricane storms, minimal hurricanes and major hurricanes (possessing a RMW within 50 km), clearly show that the near-core structure beyond the RMW for the majority of TCs is characterized by a relatively slow tangential wind decay and broad skirt of monotonically decreasing relative vorticity, in contrast to the ideal vortices compared. This is substantiated by the relatively low variability in the observed vortex behavior, in terms of the spread in the tangential wind decay exponent α for equivalent modified Rankine vortices (Table 4.1), which is less than findings in prior studies. Further, the individual cases discussed from the three TC classes, were specifically chosen to represent the full range of the relevant vortex behavior for all TCs in the sample. It must be emphasized that the individual cases were not intended to be representative of their respective TC classes, as a wide and overlapping range of vortex behavior is observed for the three intensity classes (see Fig. 4.2). In any event the most extreme case (Gilbert 1988, α=0.67), in terms of the tangential wind decay (largest

α), deviates significantly from Rankine and J ideal vortices. In other words, *no cases exhibit the rapid inverse decay of tangential wind and zero relative vorticity immediately outside the RMW, characteristic of a pure Rankine vortex.* Furthermore, *absolutely no cases agree with the extremely rapid rate of tangential wind decrease characteristic of the J vortex, with corresponding anticyclonic relative vorticity in near proximity to the RMW and its associated positive radial gradient in the vicinity of the critical radius.* These results clearly show that the pure Rankine and J ideal vortices are unrealistic and do not depict the observed slow tangential wind decay characteristic of real TCs beyond the RMW, and the associated significant skirt of relative vorticity possessing on average a negative radial gradient. Note, however, that although these unrealistic characteristics associated with the decrease of the primary vortex maximum were never observed, limited radial regions of negative vorticity and ensuing positive radial gradients were evident in some cases in which significant secondary maxima were present. This issue will be reserved for discussion in Chapter 6.

CHAPTER 5. RAPID INTENSIFICATION

5.1. Overview

The previous chapter demonstrated that the azimuthal-mean tangential wind structure beyond the RMW is decidedly non-Rankine and is characterized by a relatively slow decay in association with a broad skirt of relative vorticity. Because this inherent structural characteristic enables the TC vortex to maintain itself and withstand the destructive effects of vertical wind shear, an interesting question arises as to how the primary circulation may further influence future intensification. In particular, the central question of this chapter is addressed as to whether there exist structural features that may indicate future (or continued) rapid intensification. This is accomplished by: 1) examining the statistical relationships between the parameters that characterize the tangential wind structure (RMW, V_{max}, and the Rankine decay exponent α) and the future intensification rate and 2) comparing the tangential wind structure in the pre-hurricane stages for rapid, moderate and slowly intensifying TCs.

5.2. Tangential Wind Profile Parameters and Intensification

The first objective is to determine the stages of the TC lifecycle in which the fastest intensification occurs in the whole sample. Here, the analysis is restricted to the lowest flight-levels (700 mb and below) for cases (176) with central pressure falls and maximum wind speed increases. Figure 5.1 shows that the largest 24-hour intensification rates, in terms of large central pressure falls (ΔP_{24}) and maximum wind speed increases (ΔV_{24}), occur after a TC has attained at least tropical storm intensity (V_{max}). This is consistent with the results of Kaplan and DeMaria (2003). The largest future 24-hour intensification periods occur for strong tropical storms and minimal hurricanes while very few occur at major hurricane intensity. The latter is simply a consequence of the choice of the length of the intensification period, in this case a 24-hour intensification rate. This was chosen due to its suitability for detecting the beginning of *sustained* rapid intensification periods. Major hurricanes are very unlikely to begin or even continue to intensify for such sustained periods since they are likely close to the maximum intensity. In any event, the largest 24-hour intensification rates do not occur for the weakest and strongest TCs in the

sample, in contrast to slower intensification, which can occur at any intensity.

The axisymmetric vortex contraction that is often associated with intensification (Willoughby et al. 1982, Willoughby 1990a) suggests a possible relationship between the radius of maximum wind and the intensification rate. Figure 5.2 shows that the cases with the fastest future intensification tend to have a smaller RMW. In fact, all cases with $\Delta P_{24} > 30$ mb possessed an RMW within approximately 50 km (Fig. 5.2b). It is interesting to note that the 24-hour intensity change value of $\Delta V_{24} = 15.4$ ms^{-1} (or 30 knots), which distinguishes rapid from slower intensifying TCs in Kaplan and DeMaria (2003)'s study, appears to be an approximate cutoff point for TCs that possess an RMW size restricted to within 50 km (except for two or three cases). This particular definition, which is based on statistics, appears to have some physical basis and thus justifies its use. Although there appears to be a preferred radial scale for the most rapidly intensifying storms, many more TCs of similar RMW (and greater) intensify at a slower rate.

In addition to the TC vortex intensity and RMW, it is worth investigating whether any relationship exists between the shape of the

radial profile of tangential wind and the intensification rate. For the subset of cases (94) possessing an RMW within 50 km (conveniently including most of the rapid intensification cases), the modified Rankine decay exponent α can be estimated between 1-3 RMW distances, as in Chapter 4. The relationship with the intensification rate is depicted in Fig. 5.3. In general, there appears to be a poor correlation between both ΔV_{24}, ΔP_{24} and α. There does not appear to be a preferred range in the rates of tangential wind decay for the largest intensification rates.

The preceding analysis and discussion was intended to give a broad picture of the relationship between the intensification rate and the general characteristics of the azimuthal-mean tangential wind structure. Clearly, a poor statistical relationship exists between each of the three tangential wind profile parameters (V_{max}, RMW and α) and the future 24-hour intensification rate. However, there may be other aspects of the radial TC structure other than these three parameters that may distinguish rapidly intensifying TCs. For this reason, the actual radial profiles of tangential wind are compared in the following sections for different TC classes defined by the future intensification rate.

5.3. Intensification Categories

The preceding section provided some useful information for a definition of rapid intensification, revealing the preferred RMW size of the fastest intensifying cases which happen to conform rather nicely with the Kaplan and DeMaria (2003) criterion. Using this definition as a guide, the relationship between V_m, RMW, and ΔV_{24} is summarized in a scatter diagram (Fig. 5.4) by stratifying the cases into three intensification classes: *rapid* ($\Delta V_{24} > 15.4$), *moderate* ($7.7 < \Delta V_{24} \leq 15.4$) and *slow* ($0.0 < \Delta V_{24} \leq 7.7$). Notice that the best-track maximum wind speed V_m is employed here for TC intensity classification (Section 3.3), which is important for distinguishing different types of rapid intensifiers.

All of the *early* rapid intensification cases ($V_m < 36$ ms^{-1}, or 70 kts) preceded the largest wind speed increases and central pressure falls (not shown). The remaining cases ($V_m \geq 36$ ms^{-1}, or 70 kts) were either 1) near the onset of *late* rapid intensification or 2) had already experienced a significant period of rapid intensification, most of which were later incarnations of storms from the early rapid intensification group.

5.4. Early Rapid Intensification

5.4.1. *Onset Stage*

Consistent with the main focus of this chapter, the tangential wind structure near the onset of rapid intensification is the primary concern. This focus of this section is on the more abundant cases that began rapid intensification near the time that hurricane status was achieved. The evolution of the radial profile of tangential wind from the tropical storm stage to near peak intensity for all rapidly intensifying storms is graphically displayed in Appendix B and will be referred to throughout the remaining discussion. Similarly, Appendix C illustrates the tangential wind evolution for a few cases of slow or moderate intensification.

Five storms (Andrew 1992, Bret 1999, Diana 1984, Michelle 2001, Mitch 1998) are near their greatest 24-hour rapid intensification period just as hurricane intensity is reached with their RMW located within 50 km of the cyclone center. This is the point at which the largest pressure falls begin coinciding with the symmetric contraction and intensification of the vortex (Figs. B.1-B.5). Notice that the azimuthal-mean vortex (V_{max}) intensifies by greater than 20 ms^{-1} in all five cases, sometimes far exceeding the best track estimate.

Fortunately, there are many more cases of similar intensity and RMW to compare with that intensify at a slower rate. This is not only due to the relative rarity of rapid intensification events, but also a consequence of the greater number of flight missions during extended periods of slow intensity change. Only a single case per storm is selected for the comparison due to the similarity in radial structure for cases of similar intensity (from the same storm). The result is seven slow and seven moderate cases to compare with the five rapid cases.

For the three intensification classes, the tangential wind profile parameters along with intensity, intensity change and flight level are summarized for each case in Tables 5.1-5.3. Note that the best-track maximum wind speed V_m for all cases is very close to the minimum value required for hurricane classification. The particular cases in the moderate and slow groups were chosen this way intentionally to agree as close as possible to the narrow range in V_m exhibited by the rapid cases. This is the basis for a fair comparison among intensification classes. The flight-level maximum azimuthal-mean tangential wind speed (V_{max}) is on average less than V_m and exhibits greater variability, even at the same flight-level. The variation in the central pressure (P_c) is believed to be a consequence of the

varying pressure-wind relationships for TCs of varying size (Callaghan and Smith 1998).

Given that the various measures of intensity and range of RMW are similar for the three groups, the non-dimensional radial structure (Fig. 5.5a, 5.6a, 5.7a) and, in particular, the rate of tangential wind decay (Table 5.1) outside the RMW is compared. On average, the rapid intensifiers have the greatest tangential wind decay, but perhaps more interesting is the relatively small variability that is evident in Fig. 5.5a. Most of the moderate intensifiers possess rather flat tangential wind profiles and below average tangential wind decay (Fig. 5.6a), the notable exception being the sharply peaked profile of Lili (1996). The slow intensifiers also display large variability in the tangential wind decay (Fig. 5.7a) but in contrast to the moderate group, have more cases with larger than average rates of tangential wind decay.

For the purpose of observing other possible similarities or differences in the radial TC structure, the dimensional radial profiles of tangential wind are displayed in Fig. 5.5b, 5.6b, 5.7b. Notice that cases from the moderate and slow intensifying groups that have greatly reduced (from V_m) flight-level azimuthal-mean tangential wind speed (V_{max})

possess very flat-shaped radial profiles. In fact, this may be a consequence of a lesser degree of azimuthal symmetry in the tangential wind distribution, in which a lower V_{max} results from a largely varying maximum wind radius among the different storm quadrants. The relative disorganization of the radial structure for flat profiles is also evidenced by the presence of multiple wind maxima in some cases. In contrast, the cases from the rapid group possess relatively smooth radial profiles and V_{max} closer to the best-track estimate, possibly an indication of a greater degree of symmetry and organization of the vortex core.

5.4.2. *Tropical Storm Precursors*

The preceding discussion focused on the TC stage near minimum hurricane intensity at which the greatest future intensification occurs in terms of the symmetric vortex contraction and concomitant large pressure falls. This can be seen in the tangential wind evolution depicted in Figs. B.1-B.5. The specific radial structure observed in the five rapidly intensifying storms, in terms of the rate of tangential wind decay and suggestions of vortex organization, may at best be a necessary condition for rapid intensification. This is because similar structures were evident in

a few of the slow and moderately intensifying storms, which perhaps lack some additional ingredient that is further needed for rapid intensification.

The structure at a particular chosen instant of time thus may not reveal the whole story, whereas the structural evolution in the tropical storm stage prior to the largest intensification rates may distinguish the rapid from the slower intensifying systems. Perhaps there are features evident in the radial profile of tangential wind, such as secondary maxima, that are precursors to rapid intensification.

An interesting class of tropical storm wind profiles exhibited unusually small RMW, which is not typically associated with tropical storm structure. In fact, two of the rapid intensifiers (Andrew, Bret) and four slower intensifiers (Bob, Lili, Opal, Roxanne) possess these unusual characteristics in the tropical storm stage. For all six of these cases, flight-level data was available from a very weak stage, which is rare for the HRD archive. The azimuthal-mean vortex for all cases is shown to develop very quickly from a tropical depression or weak tropical storm characterized by a very flat profile and barely discernible wind maximum to a very coherent structure in which the RMW is very small (less than 20

km) and the radial profile is sharply peaked. The resulting tight core structure for all cases is displayed in Fig. 5.8a.

Weatherford (1989) found that rapidly deepening typhoons tended to develop small eyes (and presumably small RMW) at a very early stage, in which angular momentum is allowed to pass through the region of reduced inertial stability of the outer core and concentrate near the center. The structure and evolution in these six tropical storms is possible precursory evidence of this type of TC development. While the TC vortex continues to rapidly develop to near hurricane intensity by expanding outward slightly and growing in Andrew (Fig. B.1) and Bret (Fig. B.2), the development in the other four cases has slowed (Bob – Fig. C.1, Lili –Fig. C.2) or ceased (Opal – Fig. B.7, Roxanne – Fig. C.3) as evidence of secondary maxima appears in the outer profile. Figure 5.8b depicts the difference in structural evolution between the rapid and slow/moderate intensifiers. Andrew and Bret have rapidly intensified as the vortex contracts and grows, while the outer secondary maxima in the four other cases develops significantly as the original inner maxima is in the process of decaying or has completely died (Fig. 5.8b). The resulting profile for the latter cases is broad and flat and appears to be a consequence of slow to

moderate intensification. This is similar to the behavior of double eyewalls in intense storms (Willoughby et al. 1982, Willoughby 1990a), although here the outer wind structure is most likely to be asymmetric.

All six cases with similarly small initial vortex cores, of course, do not rapidly intensify, refuting the notion that small RMW tropical storms (and presumably early eye appearances), lead to rapid intensification. However, all six cases eventually became significant hurricanes, lending at least some credence to the idea that this type of tropical storm structure may allow for further development as a consequence of lower inertial stability in the outer core. An interesting difference between the two types is that the size of the outer circulation (ROCI, see Section 2.3) for all four slow/moderate intensifiers was initially very large (>400 km) and at least twice the size of the two rapid intensifiers (<200 km), suggesting that the relative proximity of the storm environment to the inner vortex region may influence the manner in which intensification proceeds. Despite the 150 km radial limitation of the data, the difference in vortex size may also be apparent in the actual radial profiles, with the slower intensifying TCs possessing flat or even sometimes increasing profiles in the outer vortex region well beyond the RMW.

The difference in the manner in which both types intensify appears to be in the way outer maxima interact with the primary vortex. In the case of Bret (Fig. B.2), a secondary maximum clearly "propagates" inward and appears to coalesce with the original inner maximum as rapid intensification commences. The growth and slight expansion of Andrew's wind maximum (Fig. B.1) before rapid intensification may be a result of subtle and undetectable secondary maximum in the azimuthal-mean profile. A more dramatic example of this outward expansion is the case of Mitch (Fig. B.5), in which development occurs outside the remnant core within 50 km radius. This increase in the azimuthal-mean profile is solely due to development in one particular quadrant (not shown), followed by increasingly symmetric vortex contraction and rapid intensification. On the other hand, all four of the slow/moderately intensifying storms developed significant outer maxima that appeared to interact destructively with the original small vortex core.

5.5. Late Rapid Intensification

There were only two cases of rapid intensification that began at a more advanced stage of development, both Opal (1995) and Floyd (1999) as Category 2 hurricanes. Opal (1995) developed very slowly for several days,

as discussed in the preceding section, resulting in a relatively broad radial structure prior to experiencing the greatest intensification rate of any TC in this study (Fig. B.7). Overwhelming evidence that there are no unique tangential wind characteristics that *guarantee* future rapid intensification lies in the fact that Opal's tangential wind profile remained relatively unchanged for twenty four hours prior to the onset. Floyd, on the other hand, intensified rather quickly from the tropical storm stage to strong Category 2 intensity (Fig. B.8). Floyd then weakened as the radial structure expanded (RMW near 80 km) and flattened before commencing its most rapidly intensifying period.

The radial structure of Opal and Floyd prior to rapid intensification raises an important point. The periods of slow development or weakening prior to rapid intensification led to rather broad and flat wind profiles (Figs. B.7, B.8), in contrast to the more sharply peaked profiles of the early rapid intensifiers in which there were no apparent interruptions to the intensification (Figs. B.1-B.5). Here, the general structure appears to be more of a consequence of the rate of intensification in the *prior* 12-24 hour period. Therefore, precursors that might indicate future rapid intensification may be subtle and difficult to discern in the azimuthal-

mean radial profile. However, the structural organization is likely a factor in the future intensification as well as the interaction between outer secondary maxima with the existing inner vortex core.

CHAPTER 6. DISCUSSION AND CONCLUSIONS

In this extensive flight-level observational study of the TC primary circulation, hundreds of azimuthal-mean tangential wind and relative vorticity profiles were constructed from thousands of individual radial profiles obtained from aircraft observations of Atlantic and Eastern Pacific tropical cyclones. The first part of this study emphasizes the near-core region beyond the RMW, which is important for vortex resiliency and robustness, with the purpose of identifying the mean radial structure of TCs and to compare with some commonly used ideal vortices in theoretical studies. The second part of this study primarily concerns the importance of the radial structure on rapid intensification.

6.1. Vortex Resiliency and Robustness

Mean tangential wind and relative vorticity composites, and in fact the full range of individual cases, reveal that the true underlying radial structure of TCs is distinct from the idealized vortices by the relatively slow tangential wind decrease and the associated monotonic decay of cyclonic relative vorticity in the near-core region beyond the radius of maximum wind. The characteristic broadness in the radial structure of real TCs guarantees *a strong negative radial gradient of vorticity at the*

critical radius that has recently been implicated as essential to maintaining the resiliency of the TC vortex in weak to moderately sheared environments.

According to linear VRW theory, the azimuthal-mean radial structure in the near-core region outside the RMW plays an essential role in determining the TC vortex response to vertical wind shear. Different outcomes in the vortex response to vertical shear can be expected depending on the choice of idealized vortex profile, as demonstrated by Reasor et al. (2004) and Schecter and Montgomery (2003, 2004). For a pure Rankine vortex with core Rossby number greater than unity, linear theory predicts, and numerical simulations verify, an unstable response in which the tilted vortex precesses with exponential growth in the tilt angle (Schecter and Montgomery 2004). The *positive* gradient of relative vorticity of the J vortex at the critical radius associated with the rapid tangential wind decrease and negative relative vorticity yields an unstable response in which the vortex tilt increases with time and eventually shears apart (Jones 1995, Reasor et al. 2004). The unrealistic Rankine and J vortices evidently lack the girth in the tangential wind and cyclonic relative vorticity structure that is necessary to withstand weak to

moderate vertical shear. The results of a follow-up study to Jones (1995) in fact support Reasor et al. 2004 and Schecter and Montgomery (2003), where the simulation of a *broader* version of the J vortex (not shown here) resulted in vertical coherence in the presence of sustained unidirectional vertical shear (Jones 2000). The VRW theory offers the simplest consistent explanation of the difference in vortex behavior: the further placement of the cyclonic to anticyclonic PV transition (~4 RMW) yields monotonically decreasing PV and a negative radial gradient at the critical radius.

From the perspective of dry adiabatic dynamics, the foregoing results suggest that the near-core vortex structure outside the RMW enables TCs to withstand and survive episodes of weak to moderate vertical wind shear, in contrast to the response of the unrealistic Rankine and J idealized vortices discussed. The VRW predictions concerning the relationship of vortex broadness and vortex resiliency have been broadly verified in the full physics cloud-resolving numerical simulation of Hurricane Bonnie (Braun et al. 2003). Bonnie experienced moderate to strong northwesterly shear during a portion of the intensive observation period, yet remained intact and vertically coherent. Together, these results

demonstrate that caution must be used in the type of idealized vortex specified in theoretical and modeling studies.

The conclusions thus far are based on the observed vortex behavior in the lower half of the troposphere for all cases possessing a RMW within 50 km of the center. This is a consequence of the radial and vertical limitations of the flight-level data, which preclude investigation of the TC structure for the entire vortex region. Due to the 150 km radial extent of the data, the vortex behavior of the remaining cases possessing RMW beyond 50 km is only observed to a radius less than three RMW distances. The larger the RMW, the less vortex structure information is available for the radial region sufficiently far beyond the RMW that is important for the vortex robustness, i.e., where the critical radius likely resides. The available knowledge of observed vortex structure for these larger RMW cases (not shown), however, give no indication of deviating from the results presented for the majority of cases that possess smaller RMW (within 50 km radius). In particular, the available data beyond the RMW does not reveal the exaggerated tangential wind decay and associated relative vorticity trends that would indicate unrealistic Rankine or J vortex behavior. In all likelihood, vortex robustness is an inherent

property of TCs, regardless of the size of the RMW. Further anticipated is that the vortex structure is unlike the Rankine or J vortex idealizations at upper levels. This is based on the upper-level vortex structure observed in past studies (see Section 1.4.1) and our observation that no appreciable difference in the pertinent vortex structure exists between lower and middle levels of the troposphere. For example, numerous cases in which flight missions occurred simultaneously at different altitudes did not reveal great differences in V_{max}, RMW and most importantly the radial profile shape. At the very least, the vertically averaged vortex is expected to possess the relevant structural characteristics necessary for vortex robustness and resiliency found at lower levels.

Another caveat concerns the presence of secondary maxima in the tangential wind field, as discussed in Section 4.3. The smallest scale fluctuations (<10 km) evident in the horizontal wind field would likely vanish in the azimuthal-mean for an individual storm, given a sufficient distribution of observations of an individual storm. The resultant relative vorticity profiles would reveal in most cases monotonically decaying skirts possessing clear negative radial gradients. However, significant secondary maxima that exist on a broader scale (>10 km, Samsury and Zipser 1995),

whether associated with symmetric features such as secondary eyewalls or asymmetric structures associated with spiral rainbands, will be present to some degree in the azimuthal-mean. The secondary maxima could render the TC vortex less resilient, according to the VRW theory, if the critical radius resides in the region of positive relative vorticity gradient. Adhering to the conservative estimate for the location of the critical radius (1-3 RMW), most cases in this study do not possess significant secondary maxima in this region. The current state of the VRW theory, however, does not take into account secondary maxima in the azimuthal-mean radial structure, and is reserved for future study.

Finally, the conclusions reached in this study concerning the relative broadness in the tangential wind decay and deviation from Rankine vortex behavior may appear obvious to those familiar with observations of TC structure. The presence of such unrealistic idealized profiles used in theoretical studies further begs the question of why such idealizations are used at all. The case of Jones (1995), the unrealistic profile used may have been a result of limited computing power, in which the necessity to resolve the inner vortex required a large RMW, forcing the rapid tangential wind decay to the outer boundary. Another possibility

concerns the desirable effect of conserved total angular momentum in the TC motions studies from this particular era, which requires a transition from cyclonic to anticyclonic vorticity at some radial distance in the outer vortex region. The location of the negative relative vorticity, as discussed here, was placed too close to the RMW. In many other theoretical studies, unrealistic idealizations such as Rankine or other unrealistic profiles are often used, though their use may or may not be justified. The intent of this study was thus to serve as a reminder of the inherent vortex broadness observed in real TCs, which has recently been discovered to be crucial for vortex resiliency, and to caution those who may use such unrealistic vortex idealizations in theoretical studies.

6.2. Vortex Structure and Rapid Intensification

In contrast to the vortex resiliency problem, in which the mean TC radial structure is extracted from a large number of storms and flight missions, the nature of determining whether there are structural characteristics necessary for future rapid intensification reduces to an investigation of the few TCs that experience this rare phenomenon.

A preliminary study of all intensifying cases reveals overall weak statistical relationships between the parameters that characterize the

tangential wind profile and the future 24-hour intensification rate. This means that there are no general characteristics of the radial structure, such as the radius of maximum wind and rate of tangential wind decay, that indicate that rapid intensification is guaranteed to occur. This is because some storms that intensify at a slower rate were shown to possess similar characteristics. Nevertheless, the limited numbers of cases do suggest that necessary conditions may exist for TCs that begin, or continue, to rapidly intensify. Most TCs that rapidly intensify were observed to be at least of strong tropical storm/minimal hurricane intensity. This is consistent with the theoretical results of Shapiro and Willoughby (1982) in which a more rapid evolution is expected for a stronger vortex than a weaker vortex. The TCs that began rapid intensification also possessed RMW that resided within approximately 50 km of the center, whereas storms possessing RMW larger than this radial scale at this particular stage of intensity rarely began to intensify rapidly. This restricted radial vortex scale to smaller RMWs for rapid intensifiers may be explained by the nonlinear positive feedback process arising between the increased heating efficiency of convection and increasing inertial stability both confined to a small region (Schubert and Hack 1982).

Focusing on the five cases that begin their greatest rapid intensification period as hurricane intensity is achieved, a narrow range in above-average tangential wind decay is observed; suggesting another possible necessary condition for vortex rapid intensification. A wide range in behavior was evident among the slow and moderately intensifying cases, with some cases displaying rather flat-shaped profiles (characteristic of vortex disorganization) while others possessed similar characteristics as the rapid intensifiers.

In a further attempt to distinguish rapid intensifiers, the structural *evolution* from the weak tropical storm to hurricane intensity stage reveals that some cases quickly develop a very small core structure characterized by sharply peaked radial profiles of tangential wind and unusually small RMW (within 20 km). In fact, RMW of this size are only seen at this weaker stage of intensity, or for the most intense TCs that have undergone sustained periods of rapid intensification in which the vortex core has contracted significantly. In any event, this particular class of TCs further develops by the outward expansion of the RMW, possibly a result of the emergence of secondary maxima in the tangential wind field. These secondary maxima are likely to be asymmetric features despite

their presence in the azimuthal-mean radial profiles. The TCs that further intensified rapidly tended to expand slightly as a result of secondary maxima located close to the symmetric core while the slower intensifying storms expanded greatly due to the emergence of secondary maxima located much further outward. In contrast to the rapid developers, the inner maximum appears to decay as the secondary maxima overtakes it. This may be explained by the theoretical results of Montgomery and Kallenbach (1997), in which the manner that a TC vortex intensifies depends on the relative location of localized regions of convectively induced positive PV (associated with the secondary maxima). Localized regions of positive PV introduced near the RMW contribute to intensification of the vortex, whereas the secondary tangential wind maxima increases at the expense of the original inner vortex (Moller and Montgomery 2000).

Future work of the TC structure/intensification relationship should include investigation of the interaction of asymmetric features, such as rainbands, with the vortex core. The entire horizontal wind structure must naturally be considered. Additionally, varying degrees of vortex filamentation and overall storm organization may be evident in the radial

structure and play a role in the future intensification. Although the emphasis here has focused on the kinematic structure, it is quite possible that the aforementioned sufficient conditions for rapid intensification may exist in the thermodynamic structure. In particular, the low-level equivalent potential temperature in the eye-eyewall region, in which anomalous quantities may act as a trigger for rapid intensification, has recently been suggested by Persing and Montgomery (2003).

APPENDIX A. IDEALIZED VORTEX PROFILES

The four idealized tangential wind and relative vorticity profiles discussed in this paper are presented here in non-dimensional form. The radius r, tangential wind V and relative vorticity ζ are expressed in terms of their scales and non-dimensional counterparts:

$$r = RMW\ r', \quad V = V_{\max} V', \quad \zeta = \frac{V_{\max}}{RMW}\zeta'.$$

The basic scales used are the maximum tangential wind speed $V_{\max}$ and the RMW. The scale for the relative vorticity is *derived.* For notational convenience, the primes are dropped in the following non-dimensional equations.

(a) Modified Rankine Vortex

$$V(r) = \begin{cases} r & r \le 1 \\ r^{-\alpha} & r > 1 \end{cases} \tag{A1}$$

$$\zeta(r) = \begin{cases} 2 & r \le 1 \\ (1-\alpha) r^{-(1+\alpha)} & r > 1 \end{cases} \tag{A2}$$

where $0 \le \alpha \le 1$. A pure Rankine vortex, where $\alpha = 1$, is simply

$$V(r) = \begin{cases} r & r \le 1 \\ r^{-1} & r > 1 \end{cases} \tag{A3}$$

$$\zeta(r) = \begin{cases} 2 & r \le 1 \\ 0 & r > 1 \end{cases} \tag{A4}$$

(b) Rankine-with-skirt (RWS) Vortex

$$V(r)=\begin{cases} r & r\le 1 \\ \varepsilon r(1-\dfrac{2r}{3\alpha})+C_1 & 1<r\le\alpha \\ \dfrac{C_2}{r} & r>\alpha \end{cases} \tag{A5}$$

$$\zeta(r)=\begin{cases} 2 & r\le 1 \\ 2\varepsilon(1-\dfrac{r}{\alpha}) & 1<r\le\alpha \\ 0 & r>\alpha \end{cases} \tag{A6}$$

where

$$C_1=1-\varepsilon(1-\frac{2}{3\alpha}),\qquad C_2=C_1+\frac{\varepsilon\alpha^2}{3},$$

and $\varepsilon << 1$ and $\alpha > 1$. These parameters are set to $\varepsilon = 0.0498$ and $\alpha = 2$ as in Schecter and Montgomery (2003).

(c) Gaussian Vortex

$$V(r)=\frac{1+\sigma^{-2}}{r}[1-\exp(-\sigma^2 r^2/2)] \tag{A7}$$

$$\zeta(r)=(1+\sigma^2)\exp(-\sigma^2 r^2/2) \tag{A8}$$

where $\sigma \approx 1.58520$ satisfies the transcendental relation, $\exp(\sigma^2/2)-\sigma^2-1=0$.

(d) J vortex[2]:

$$V(r) = \frac{C_0 r(a + 3br^4)}{(1 + ar^2 + br^6)^2} \tag{A9}$$

$$\zeta(r) = \frac{2C_0[a + 9br^4 - r^2(a + 3br^4)^2 + 4b^2r^{10}]}{(1 + ar^2 + br^6)^3} \tag{A10}$$

where

$$C_0 = \frac{(1 + a + b)^2}{a + 3b}.$$

As specified in Smith (1990) and Jones (1995), $a = 0.3398$ and $b = 5.377 \times 10^{-4}$.

[2] Note that the original tangential wind formulation from Jones (1995) was derived from the Smith (1990) streamfunction, $\psi(r) \propto (1 + ar^2 + br^6)^{-1}$. The "3" in the numerator above was given as "5/2" in their Eq. (1), an apparent typographical error (Reasor et al. 2004). The formulation, however, was implemented correctly in the model code used in Jones (1995) (P. Reasor, 2003, personal communication).

APPENDIX B. RAPID TC VORTEX EVOLUTION

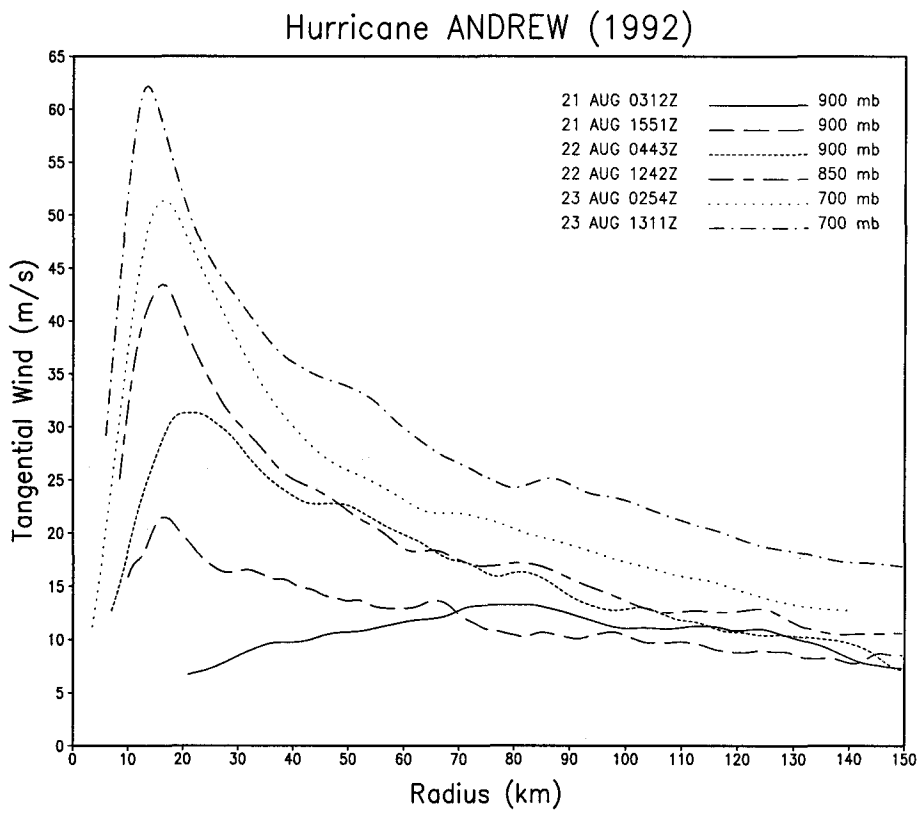

Figure B.1. The evolution of the radial structure of the low-level azimuthal-mean tangential velocity for hurricane Andrew (1992).

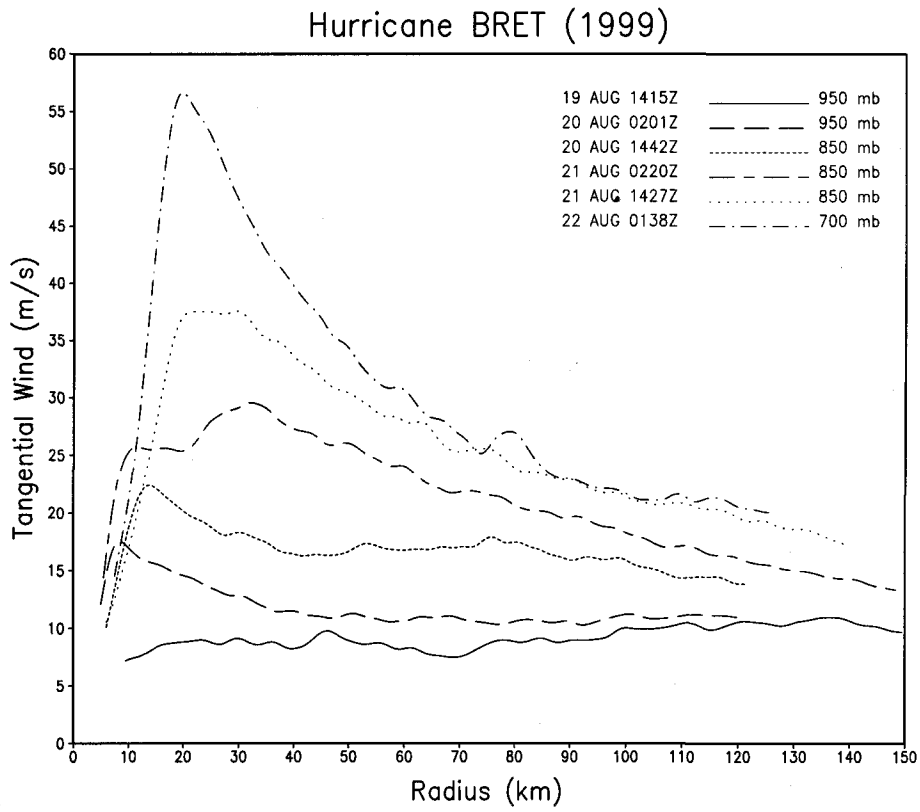

Figure B.2. The evolution of the radial structure of the low-level azimuthal-mean tangential velocity for hurricane Bret (1999), at approximately 12-hour intervals.

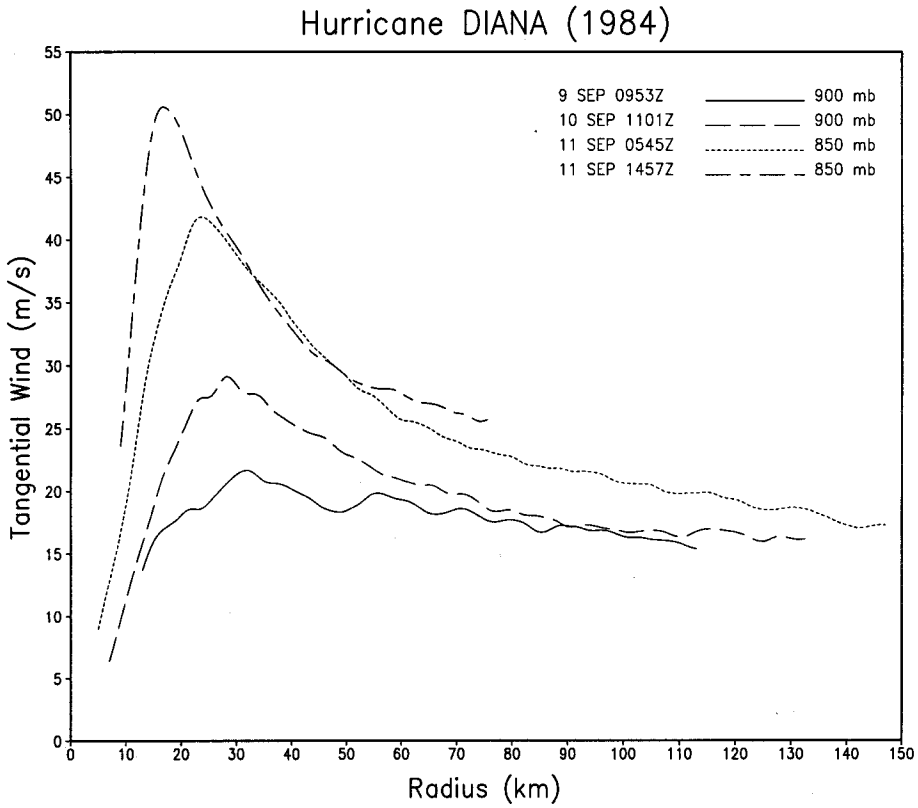

Figure B.3. The evolution of the radial structure of the low-level azimuthal-mean tangential velocity for hurricane Diana (1984).

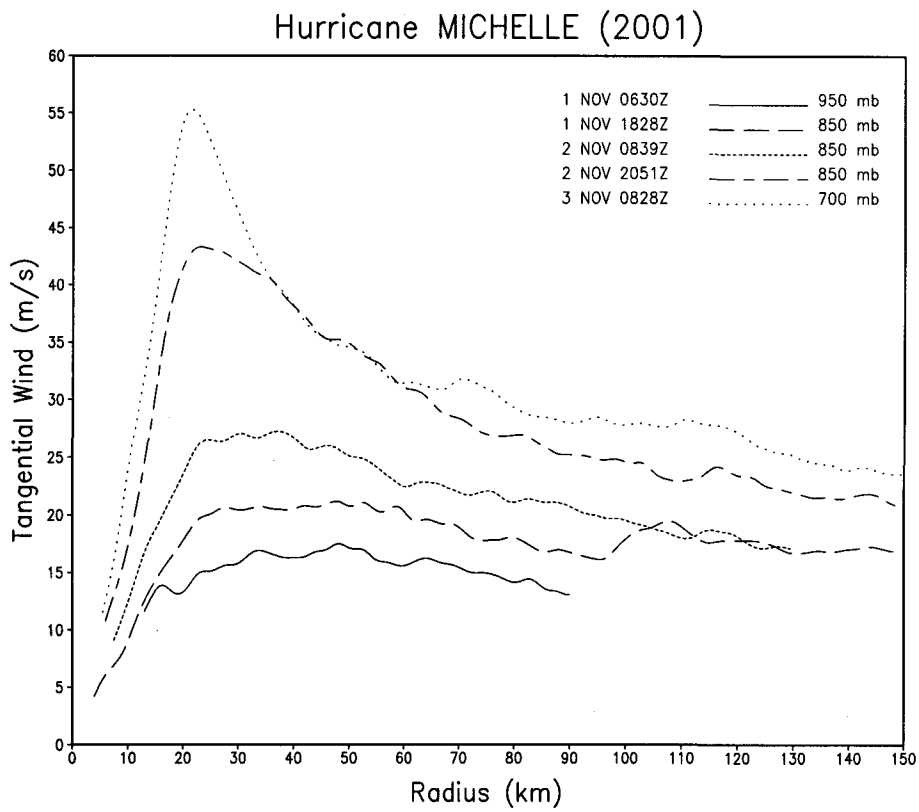

Figure B.4. The evolution of the radial structure of the low-level azimuthal-mean tangential velocity for hurricane Michelle (2001), at approximately 12-hour intervals.

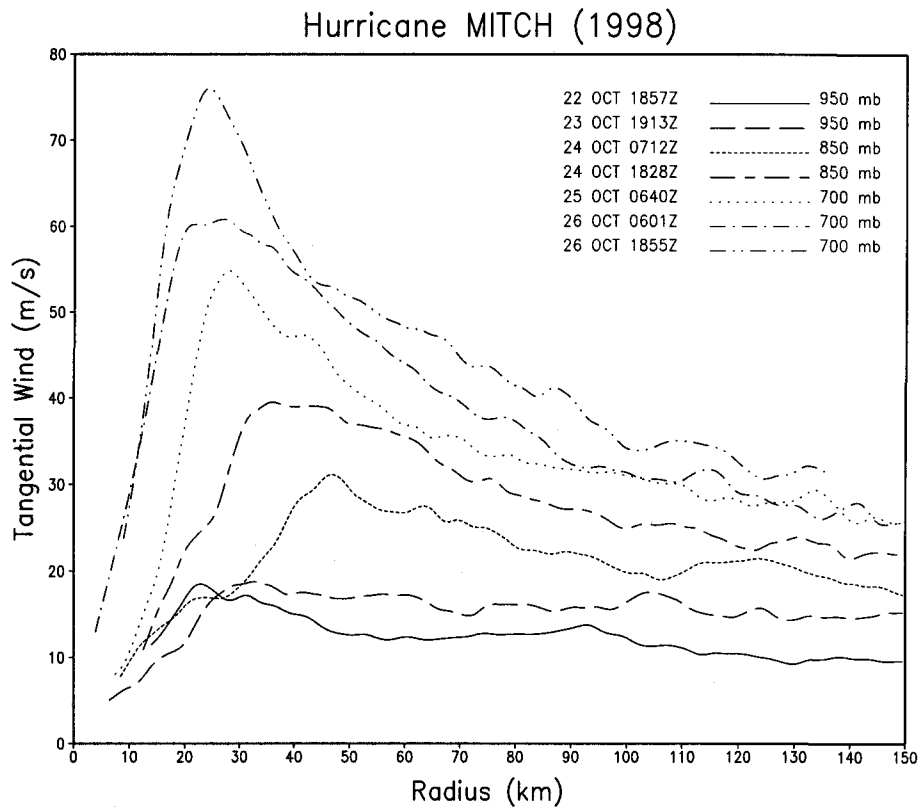

Figure B.5. The evolution of the radial structure of the low-level azimuthal-mean tangential velocity for hurricane Mitch (1998), at approximately 12-hour intervals.

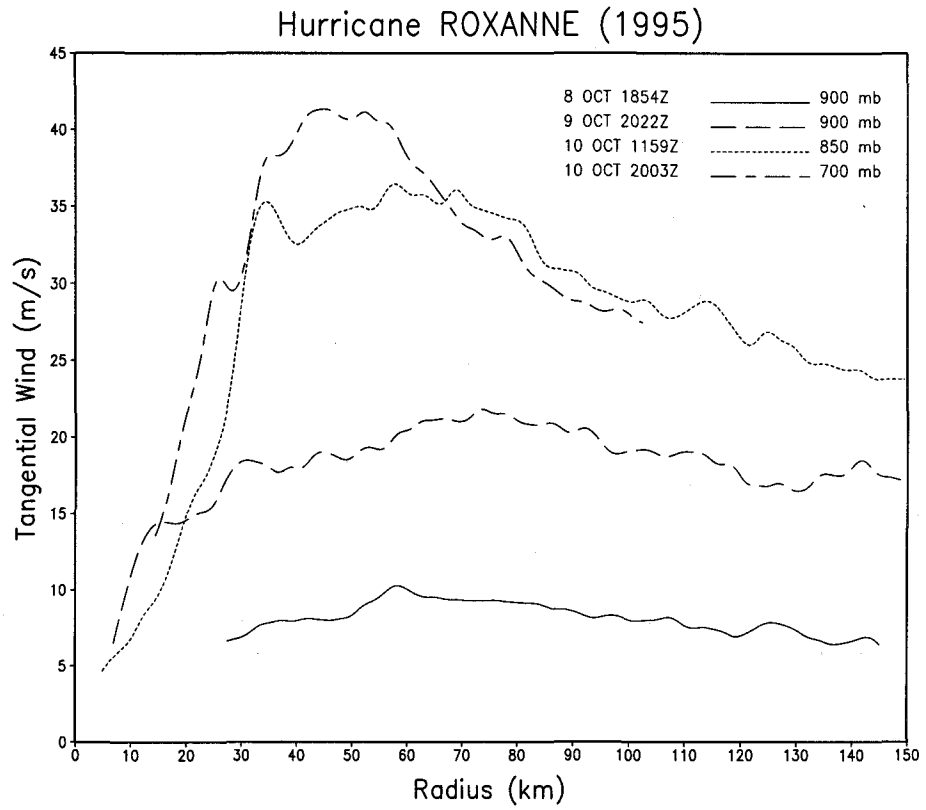

Figure B.6. The evolution of the radial structure of the low-level azimuthal-mean tangential velocity for hurricane Roxanne (1995).

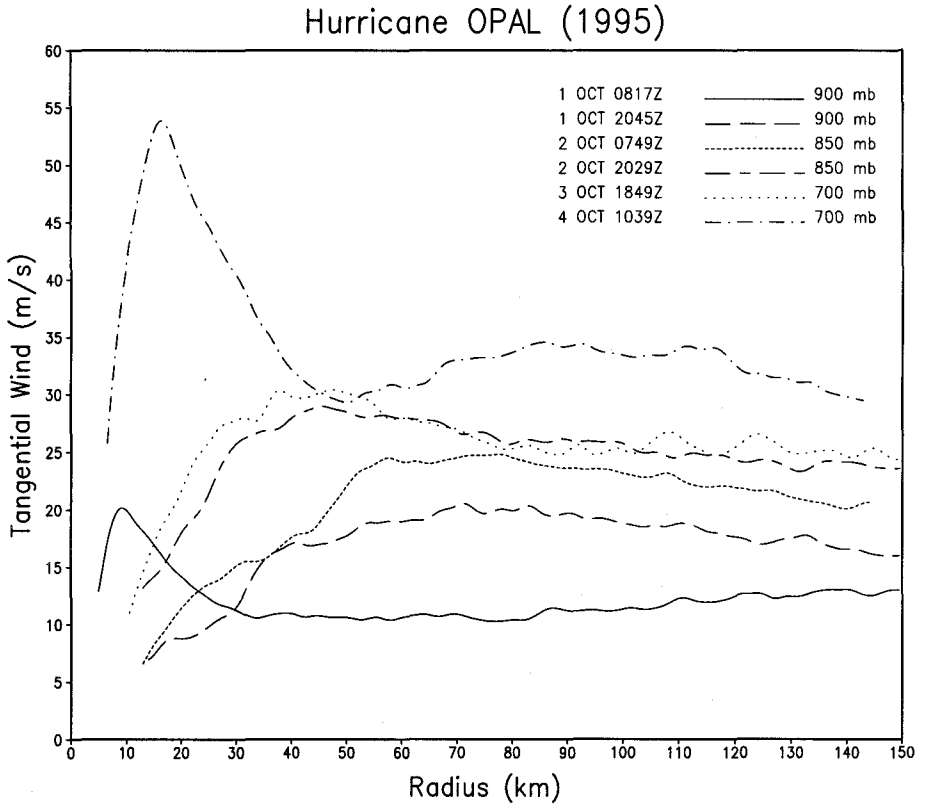

Figure B.7. The evolution of the radial structure of the low-level azimuthal-mean tangential velocity for hurricane Opal (1995).

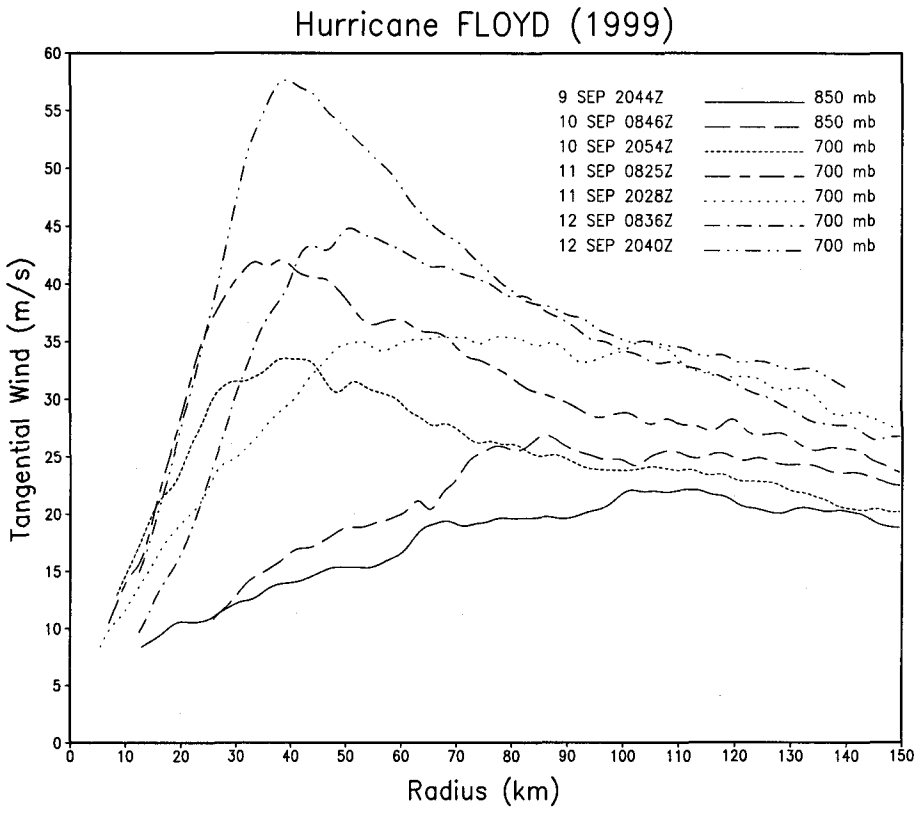

Figure B.8. The evolution of the radial structure of the low-level azimuthal-mean tangential velocity for hurricane Floyd (1999).

APPENDIX C. MODERATE/SLOW TC VORTEX EVOLUTION

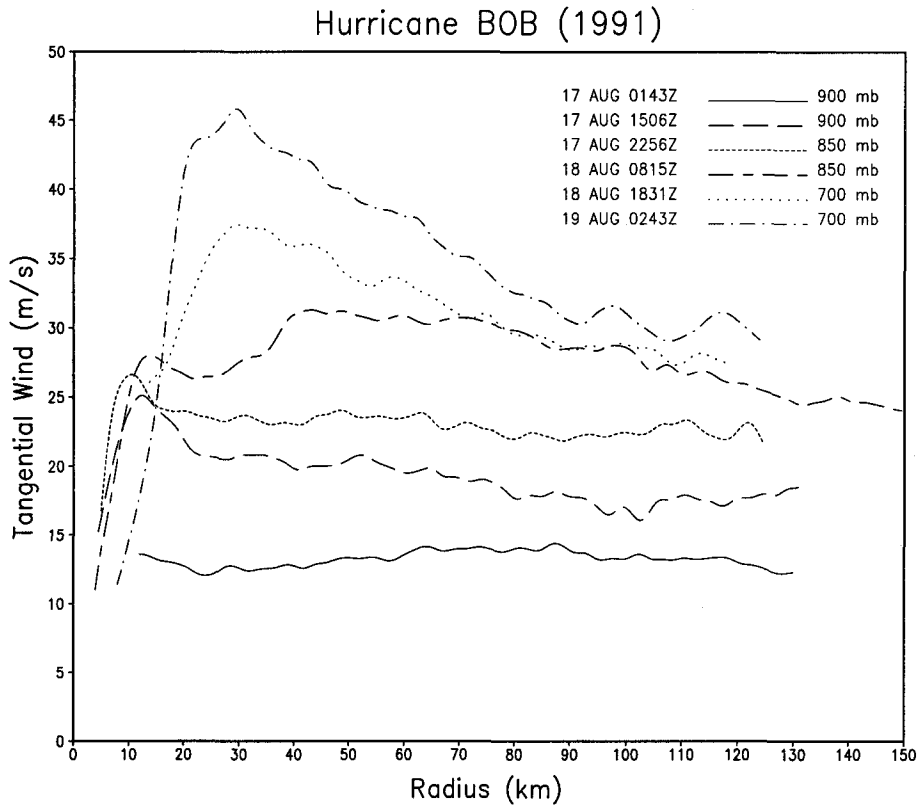

Figure C.1. The radial structural evolution for the low-level azimuthal-mean tangential wind for hurricane Bob (1991).

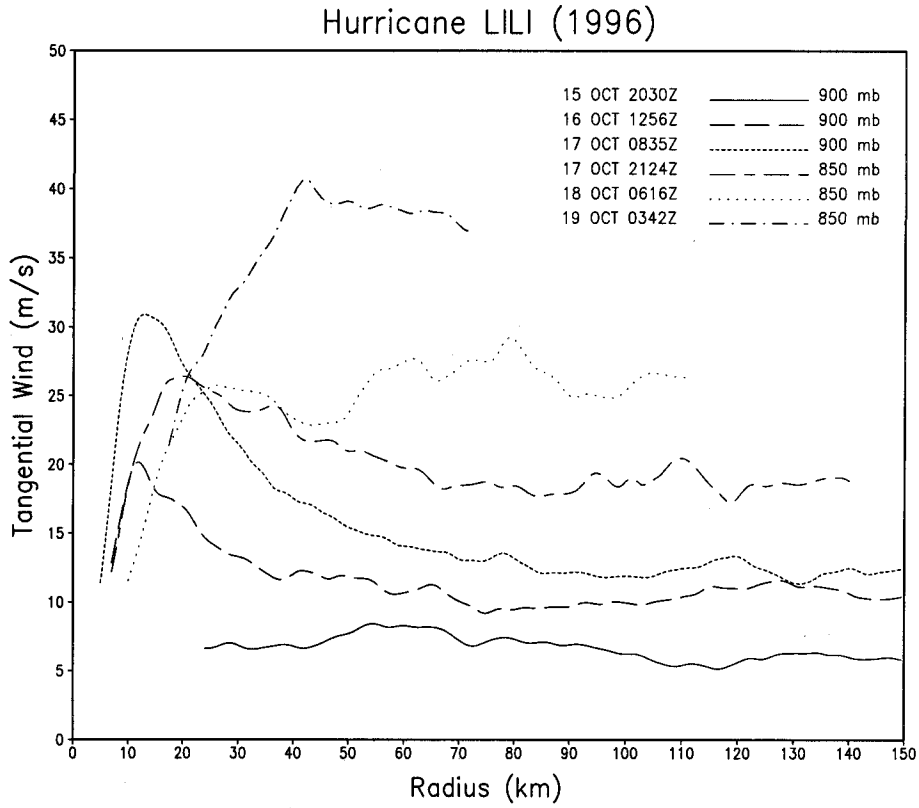

Figure C.2. The radial structural evolution for the low-level azimuthal-mean tangential wind for hurricane Lili (1996).

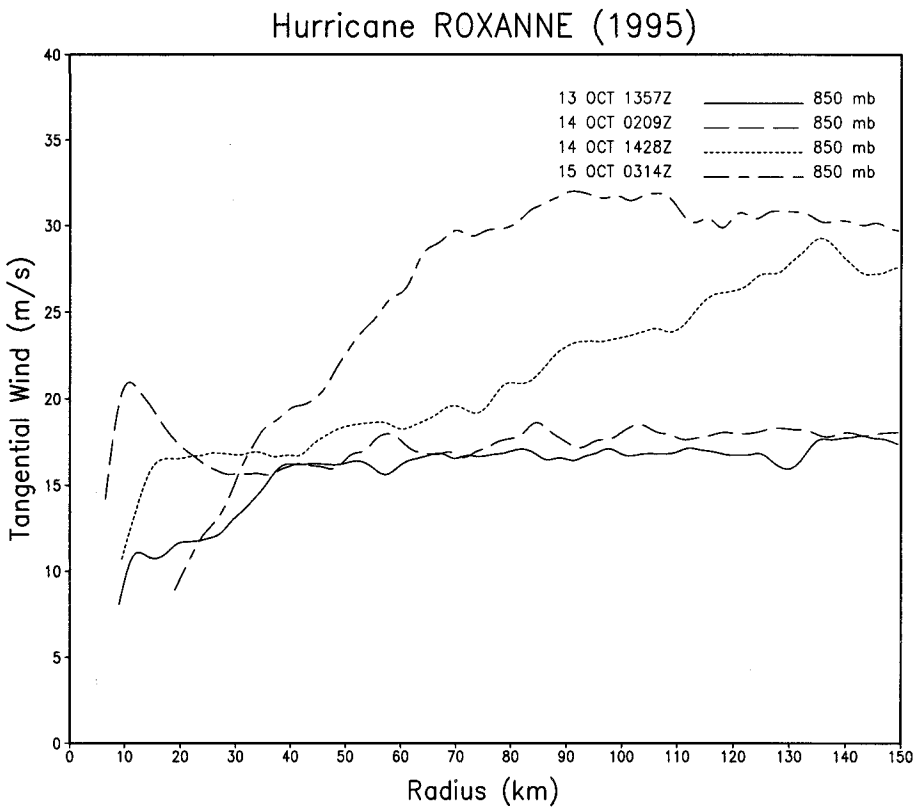

Figure C.3. The radial structural evolution for the low-level azimuthal-mean tangential wind for hurricane Roxanne (1995).

Table 4.1. Modified Rankine tangential wind decay (α) statistics for azimuthal-mean radial profiles calculated from flight-level observations of TCs possessing RMW within 50 km. The tangential wind profiles are stratified by their maximum value (V_{max}) into three intensity classes (columns 1 and 2). Column 3 gives the number of profiles and the number of storms in parentheses. Column 4 shows the mean and standard deviation of α for the 'best-fit' modified Rankine profile.

Category	V_{max} range (ms^{-1})	Observed vortex profiles (storms)	Mean (std. dev.) decay exponent
Pre-hurricane	10 - 30	75 (32)	0.30 (0.13)
Minimal Hurricane	30 - 50	108 (40)	0.35 (0.13)
Major Hurricane	50 - 76	72 (27)	0.48 (0.11)
All TCs	10 - 76	255 (53)	0.37 (0.14)

Table 5.1. Tangential wind profile parameters, intensity and intensification characteristics for five rapidly intensifying TCs near hurricane intensity, classified by the NHC best-track maximum sustained wind speed (V_m), prior to the largest 24-hour intensification rates (ΔV_{24}). Estimated values for associated minimum central pressure (Pc), maximum azimuthal-mean tangential velocity (V_{max}) and its radius (RMW), and Rankine decay parameter (α) are obtained at the midpoint of each flight mission.

Storm (year)	Flight level (mb)	P_c (mb)	V_m (ms^{-1})	V_{max} (ms^{-1})	ΔV_{24} (ms^{-1})	RMW (km)	α
Andrew (1992)	900	995	32.4	31.3	32.4	21.5	0.47
Bret (1999)	850	982	35.4	29.5	27.2	32.0	0.41
Diana (1984)	900	992	33.0	29.1	17.0	28.5	0.44
Michelle (2001)	850	984	33.1	27.2	23.1	37.0	0.38
Mitch (1998)	850	989	34.4	31.1	20.6	47.0	0.47

Table 5.2. Tangential wind profile parameters, intensity and intensification characteristics for five moderately TCs near hurricane intensity, classified by the NHC best-track maximum sustained wind speed (V_m), prior to the 24-hour intensity change (ΔV_{24}). Estimated values for associated minimum central pressure (Pc), maximum azimuthal-mean tangential velocity (V_{max}) and its radius (RMW), and Rankine decay parameter (α) are obtained at the midpoint of each flight mission.

Storm (year)	Flight level (mb)	P_c (mb)	V_m (ms^{-1})	V_{max} (ms^{-1})	ΔV_{24} (ms^{-1})	RMW (km)	α
Alicia (1983)	850	987	36.2	31.0	14.4	36.5	0.34
Bertha (1996)	700	983	36.0	30.0	15.4	35.5	0.19
Bob (1991)	850	981	35.5	26.6	12.3	10.5	0.11
Bonnie (1998)	900	990	34.6	23.8	12.9	39.5	0.07
Danielle (1998)	850	989	33.4	24.5	11.8	49.5	0.25
Lili (1996)	900	989	31.9	30.9	8.7	13.0	0.50
Opal (1995)	850	971	34.5	28.9	12.3	45.5	0.16

Table 5.3. Tangential wind profile parameters, intensity and intensification characteristics for five slowly intensifying TCs near hurricane intensity, classified by the NHC best-track maximum sustained wind speed (V_m), prior to the 24-hour intensity change (ΔV_{24}). Estimated values for associated minimum central pressure (Pc), maximum azimuthal-mean tangential velocity (V_{max}) and its radius (RMW), and Rankine decay parameter (α) are obtained at the midpoint of each flight mission.

Storm (year)	Flight level (mb)	P_c (mb)	V_m (ms^{-1})	V_{max} (ms^{-1})	ΔV_{24} (ms^{-1})	RMW (km)	α
Dennis (1999)	850	991	33.4	21.0	3.6	46.0	0.14
Emily (1993)	850	977	36.0	37.0	6.2	46.5	0.50
Erin (1995)	850	990	37.1	24.9	1.5	44.5	0.25
Fran (1996)	850	981	33.4	31.5	5.1	41.5	0.38
Iris (1995)	850	984	31.7	28.9	6.2	29.0	0.40
Marilyn (1995)	700	984	36.0	31.1	7.2	27.0	0.49
Michael (2000)	950	988	33.4	27.9	2.6	40.5	0.40

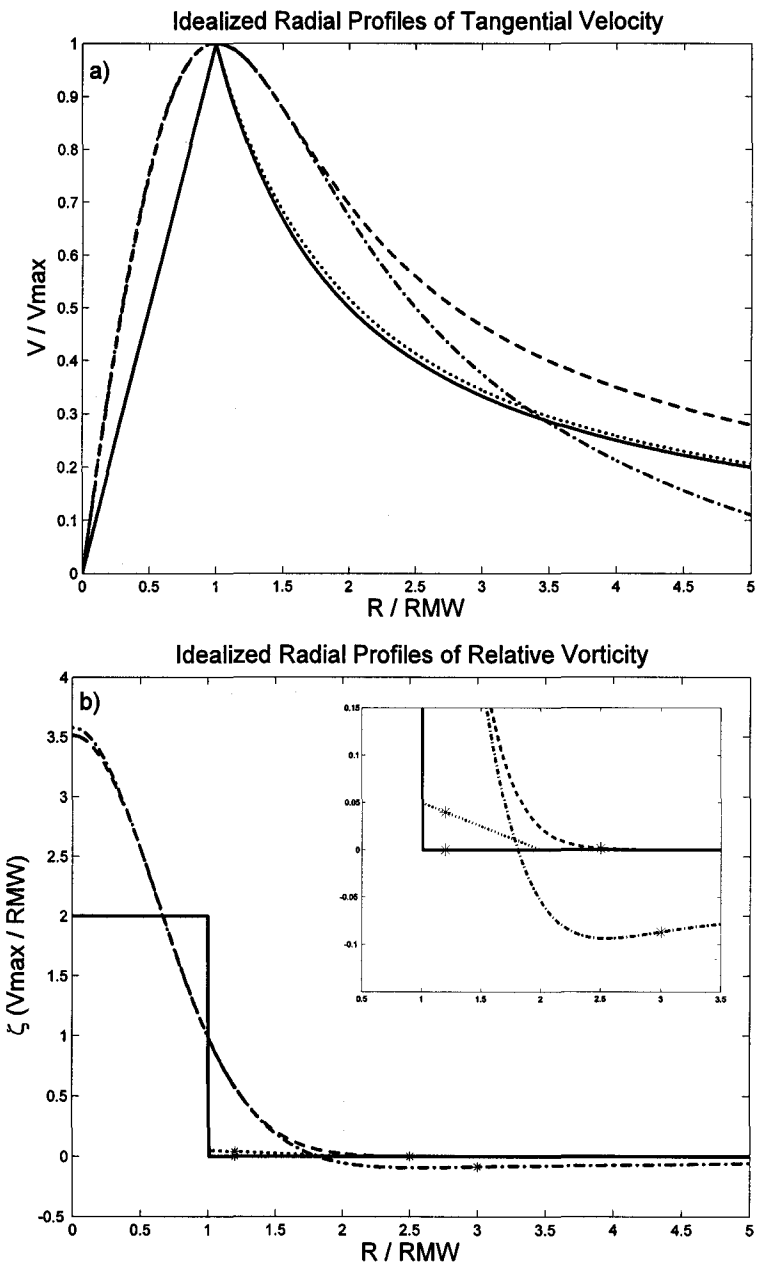

Figure 1.1. Non-dimensional radial profiles of (a) tangential velocity and (b) relative vorticity for the Rankine (solid), Rankine-with-skirt (dotted), Gaussian (dashed) and J (dash-dot) ideal vortices. The critical radii are indicated by the star symbol. The relative vorticity inset shows an expanded view of the 0.5-3.5 RMW radial region where the critical radii reside. The scaling parameters are the maximum tangential velocity (V_{max}) and its radial location (RMW). The analytic formulations for the idealized vortex profiles are given in Appendix A.

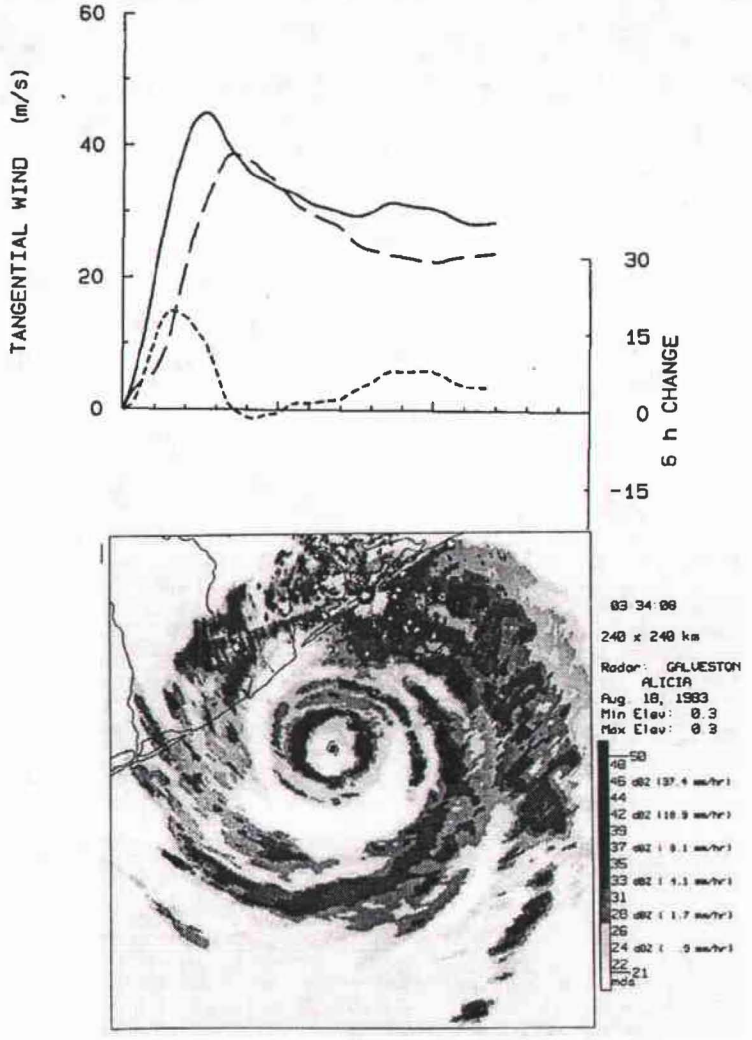

Figure 1.2. Upper panel: Evolution of the radial distribution of the 850 mb axisymmetric tangential velocity in hurricane Alicia on 17 Aug 1983 between 1159Z (long dash) and 1818Z (solid). The 6-hour tangential wind change is denoted by the short-dashed curve. Lower panel: Single sweep from the Galveston WSR-57 radar showing inner and outer eyewalls associated with their respective primary and secondary wind maxima (from Willoughby 1990a).

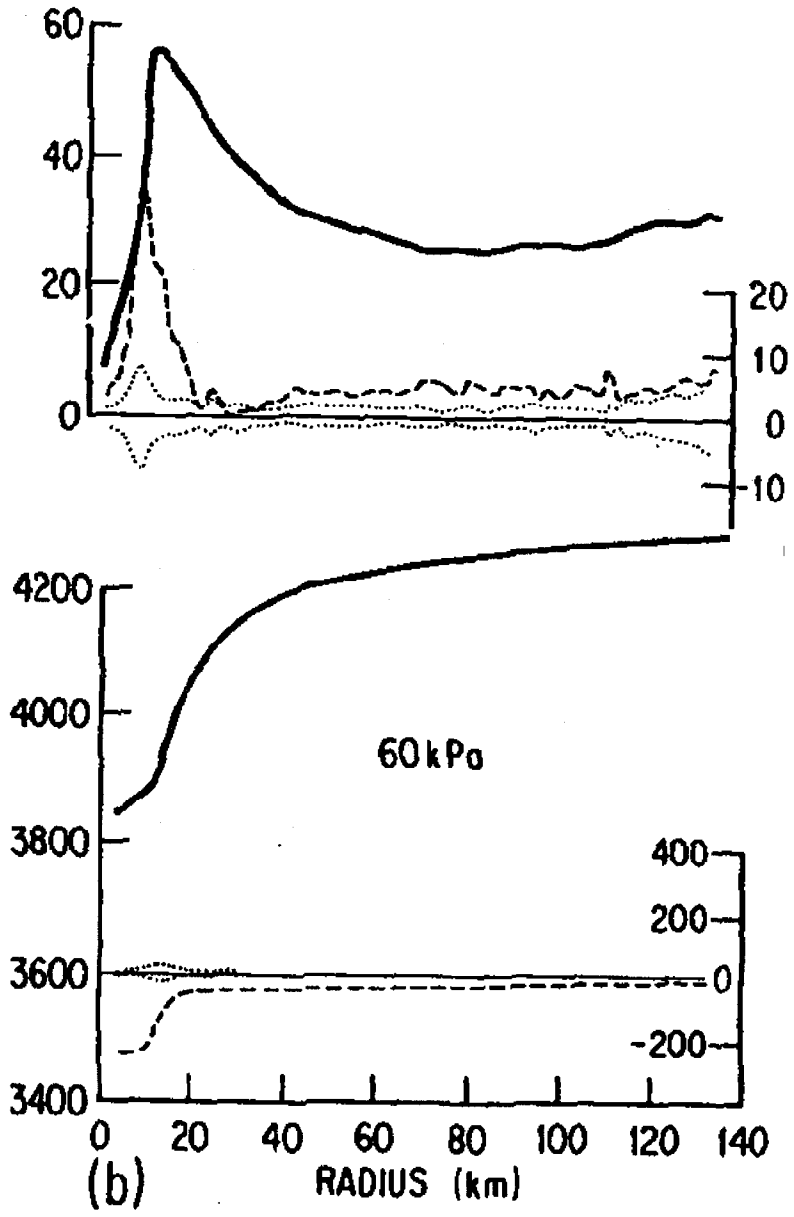

Figure 1.3. Upper panel: Radial profiles of estimated 600 mb tangential wind (solid), 6-hour tangential wind change (dashed) and RMS error (dotted) for hurricane Allen on 08 August 1980 at 2030 GMT. Lower panel:Same as upper panel, except for geopotential height (from Willoughby et al. 1982).

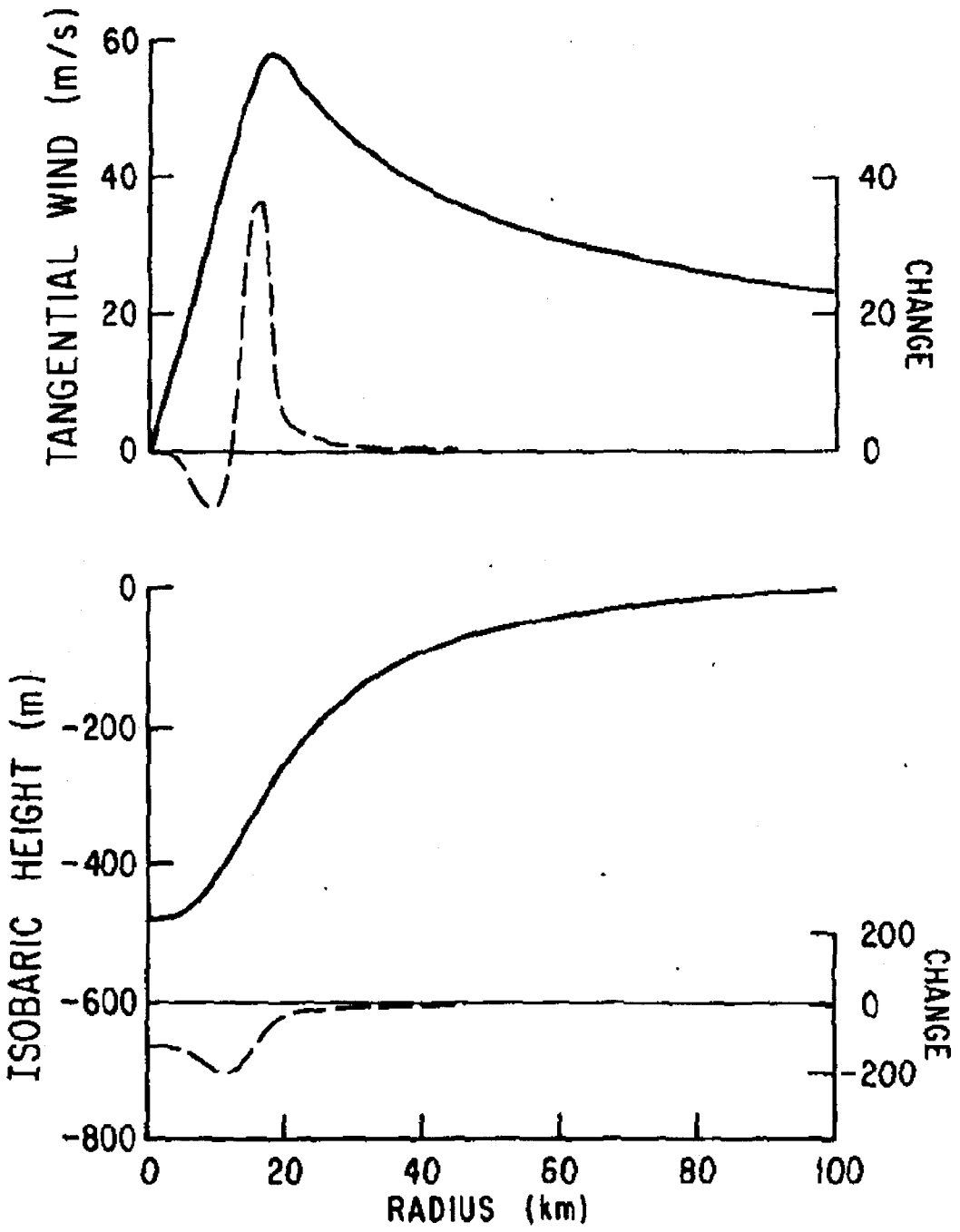

Figure 1.4. Upper panel: Tangential wind tendency (dashed) calculated from the Shapiro and Willoughby (1982) model (at 3.75 km altitude) assuming a vortex profile (solid) and heat source similar to hurricane Allen on 8 August 1980 (see Fig. 1.3). Lower panel: Same, except for isobaric height anomaly. From Willoughby et al. 1982.

a)

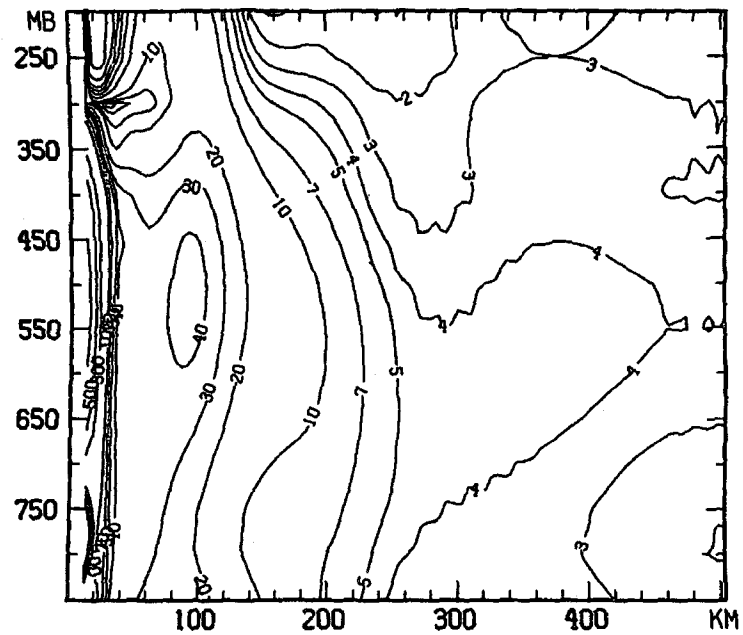

b)

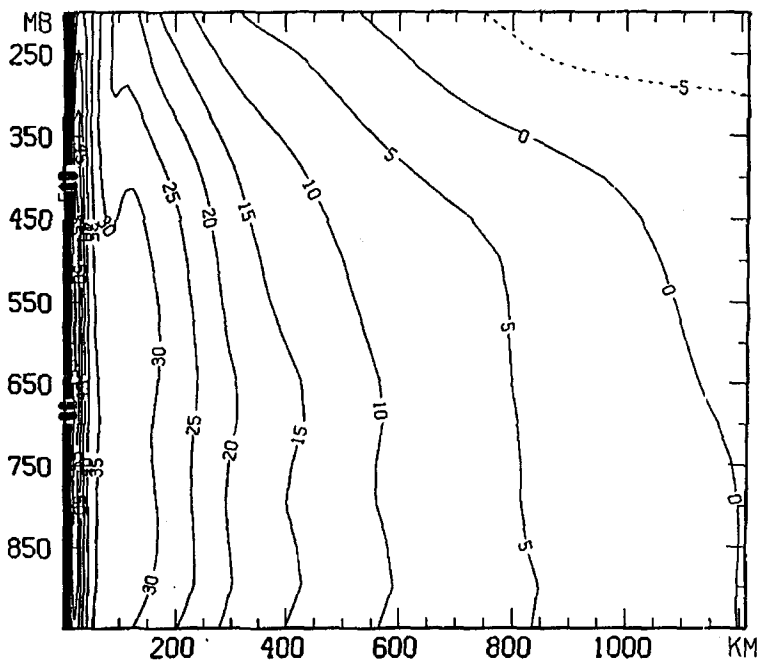

Figure 1.5. Radial-height cross-sections of hurricane Gloria's (1985) azimuthal-mean a) Rossby Ertel potential vorticity (10^{-7} m^2 s^{-1} K kg^{-1}) (from Shapiro and Franklin 1995) and b) tangential wind (m s^{-1}) (from Franklin et al. 1993).

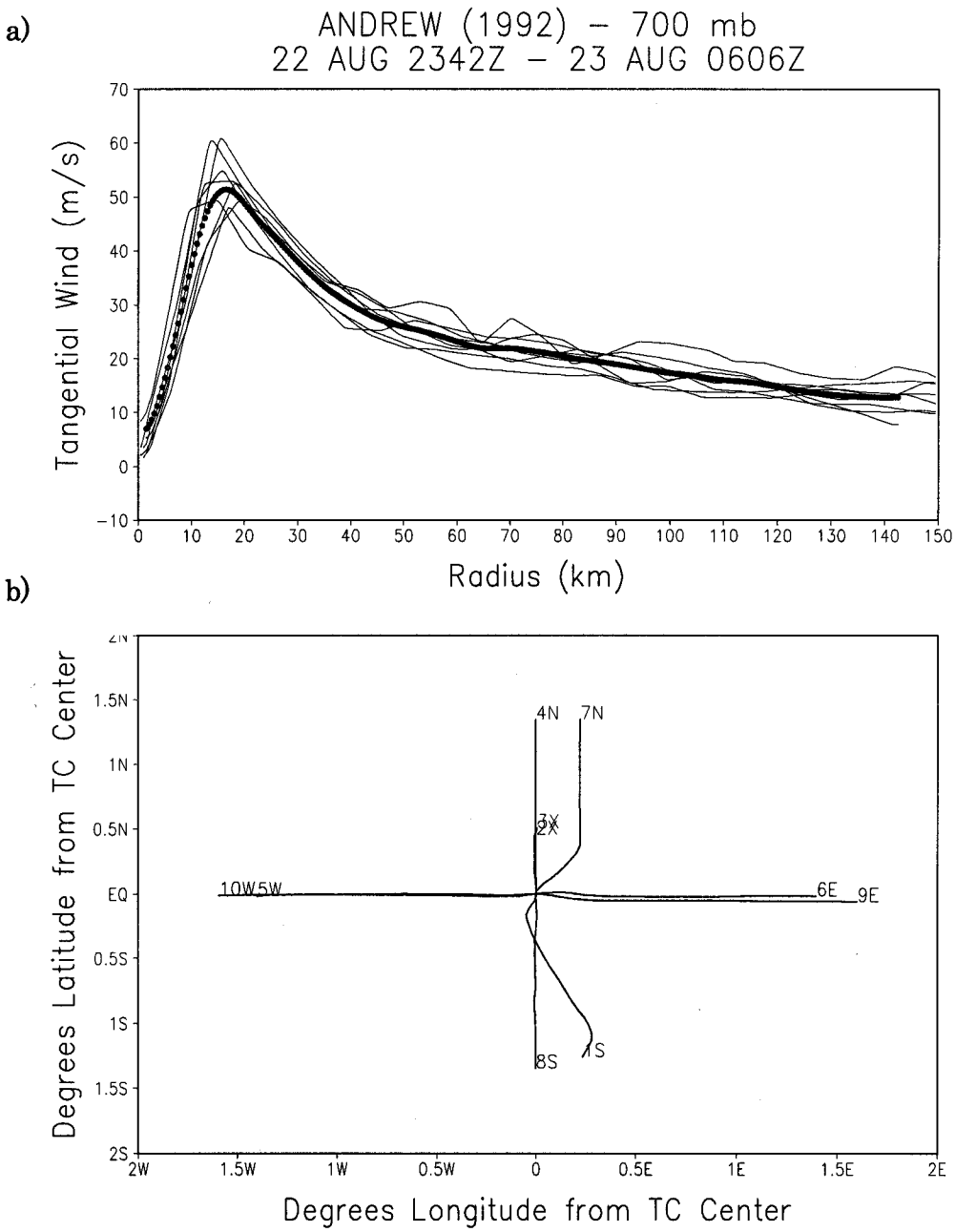

Figure 3.1 a) Individual radial profiles (thin lines) and azimuthal-mean (solid circles) tangential velocity and b) radial flight legs relative to the storm center of hurricane Andrew (1992). The radial legs are numbered in order of data sampling with cardinal direction indicated. 'X' indicates removal of the radial leg from the azimuthal-mean calculation process.

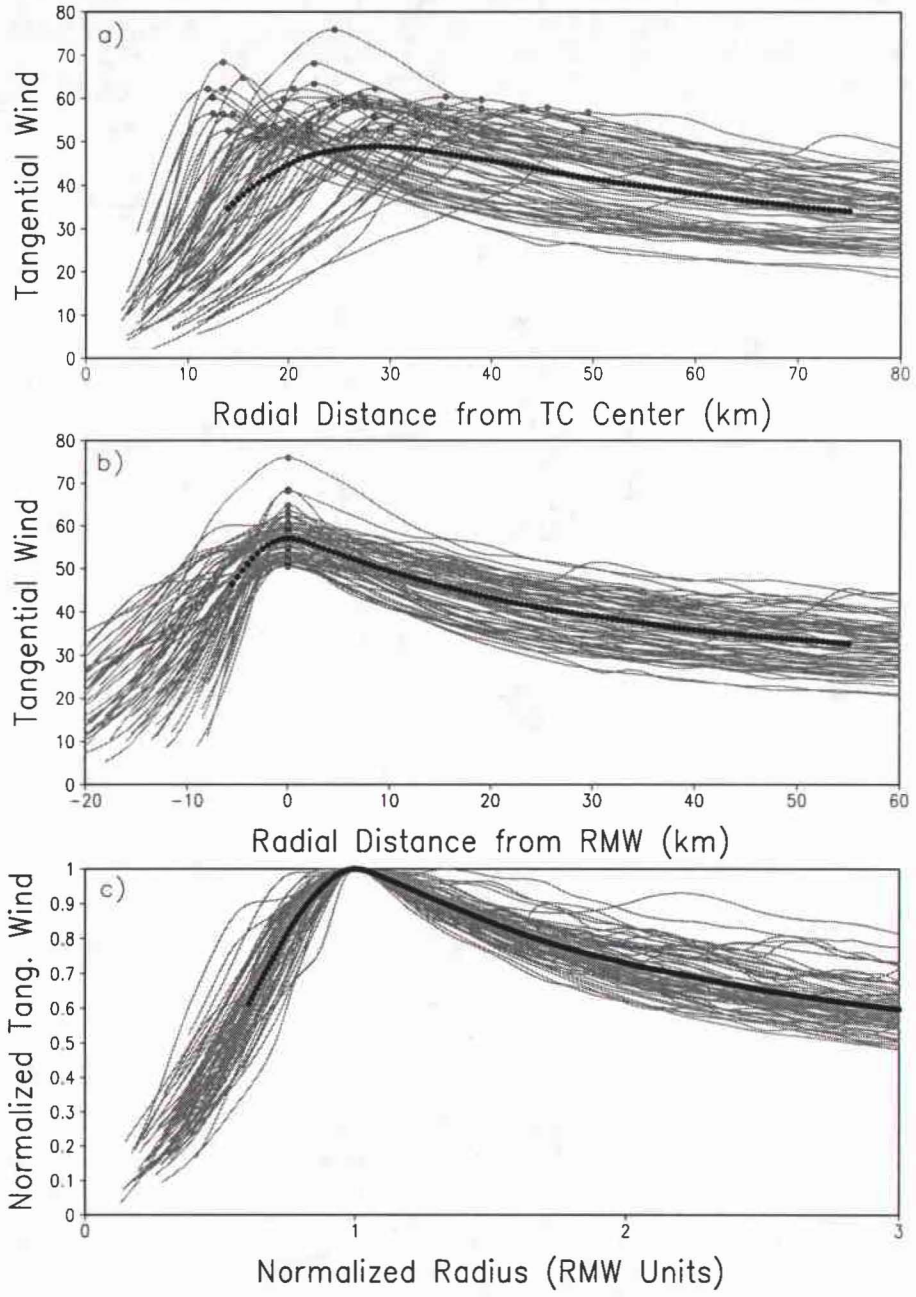

Figure 3.2. Radial profiles of azimuthal-mean tangential wind (thin lines) from 72 flight missions into major hurricanes are overlaid with the mean composite profile (solid circles). Tangential wind values (m s^{-1}) are averaged with respect to a) radial distance (km) from storm center b) radial distance (km) from radius of maximum wind (RMW). c) Normalized tangential wind values are expressed and averaged with respect to a non-dimensional radius (RMW units).

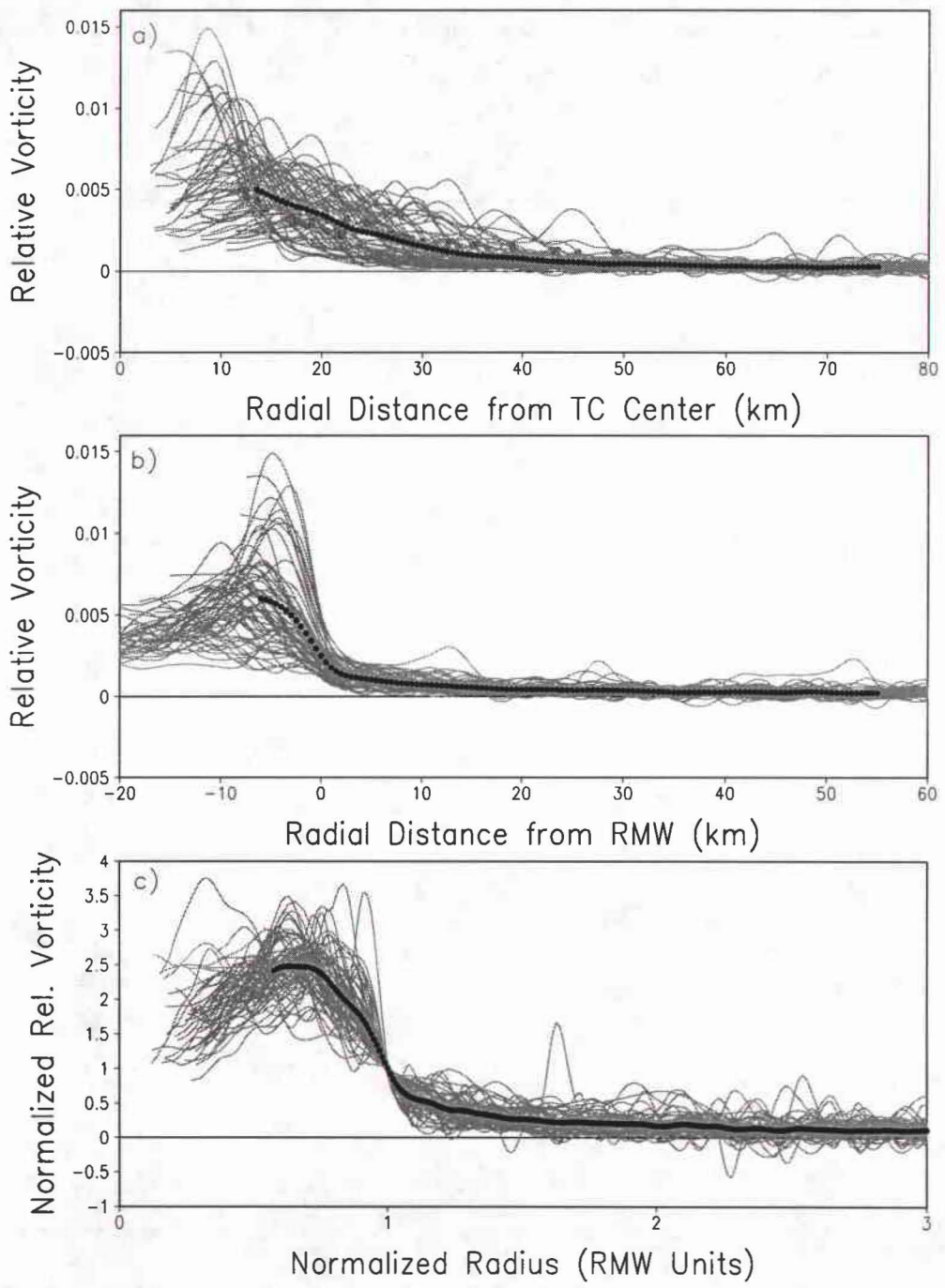

Figure 3.3. Same as Fig. 3.2 except for relative vorticity.

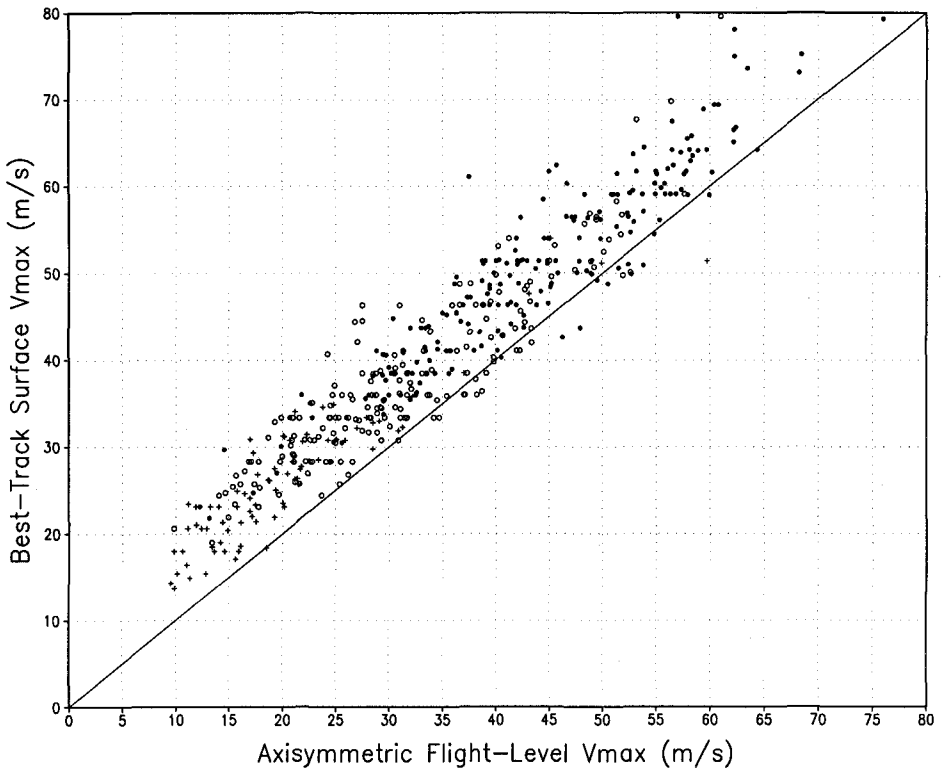

Figure 3.4. Scatter diagram of NHC best-track maximum sustained wind speed (V_m) and estimated maximum azimuthal-mean tangential velocity (V_{max}) for flight missions at the 700 mb (solid circle), 850 mb (open circle) and 900 mb (cross-hair). The straight line indicates equality of the two parameters.

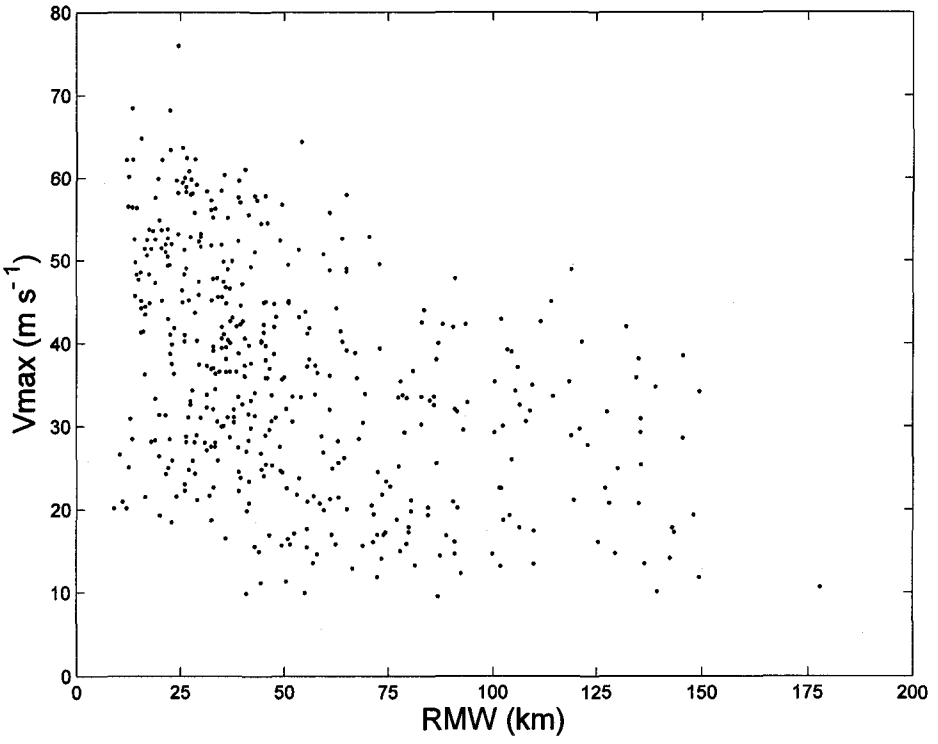

Figure 4.1. Relationship between the maximum azimuthal-mean tangential velocity (V_{max}) and its radial location (RMW). Each datum represents an azimuthal-mean vortex profile calculated from flight-level observations obtained during a flight mission (450 total).

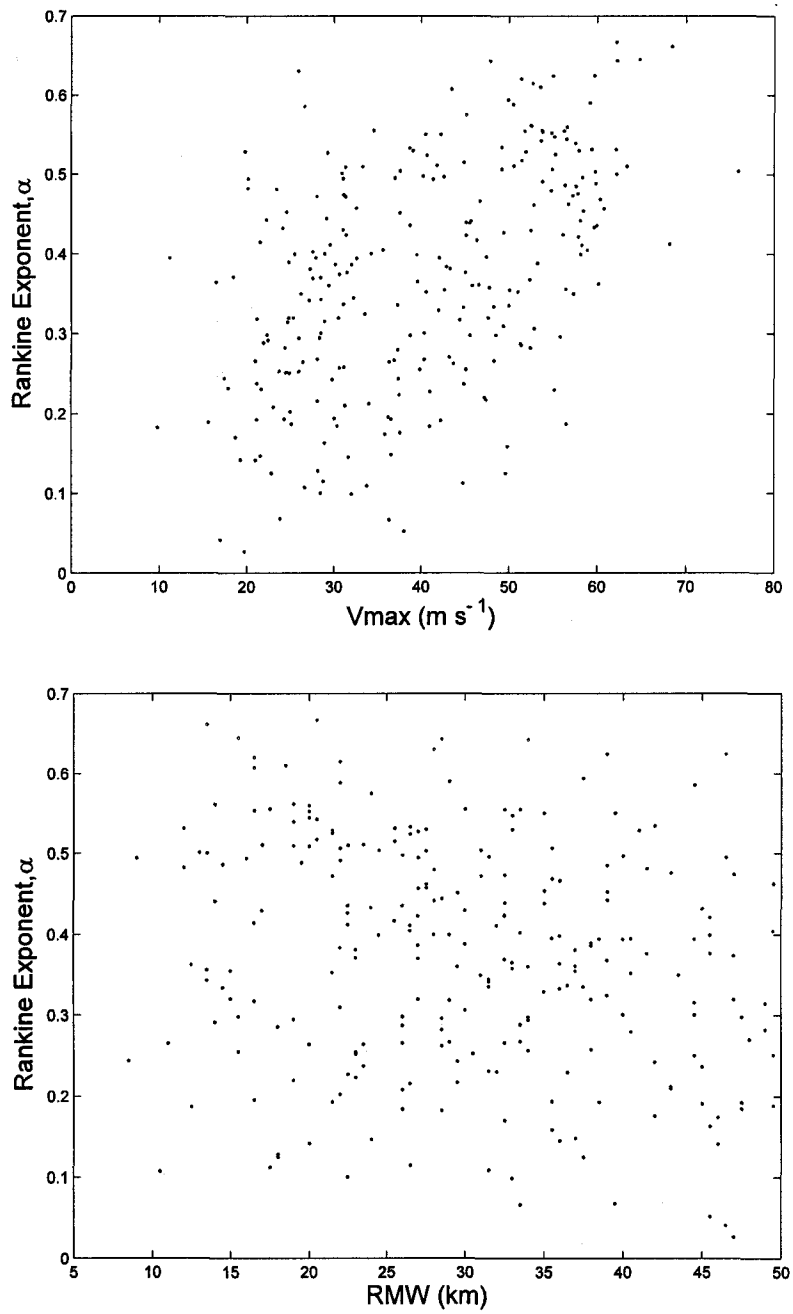

Figure 4.2. Relationship between the modified Rankine decay parameter (α) and the maximum azimuthal-mean tangential velocity (V_{max}) (upper panel) and its radial location (RMW) (lower panel). Each data point represents an azimuthal-mean vortex profile calculated from flight-level observations obtained during a single mission. The sample is restricted to individual cases for which RMW $\leq$ 50 km (255 total).

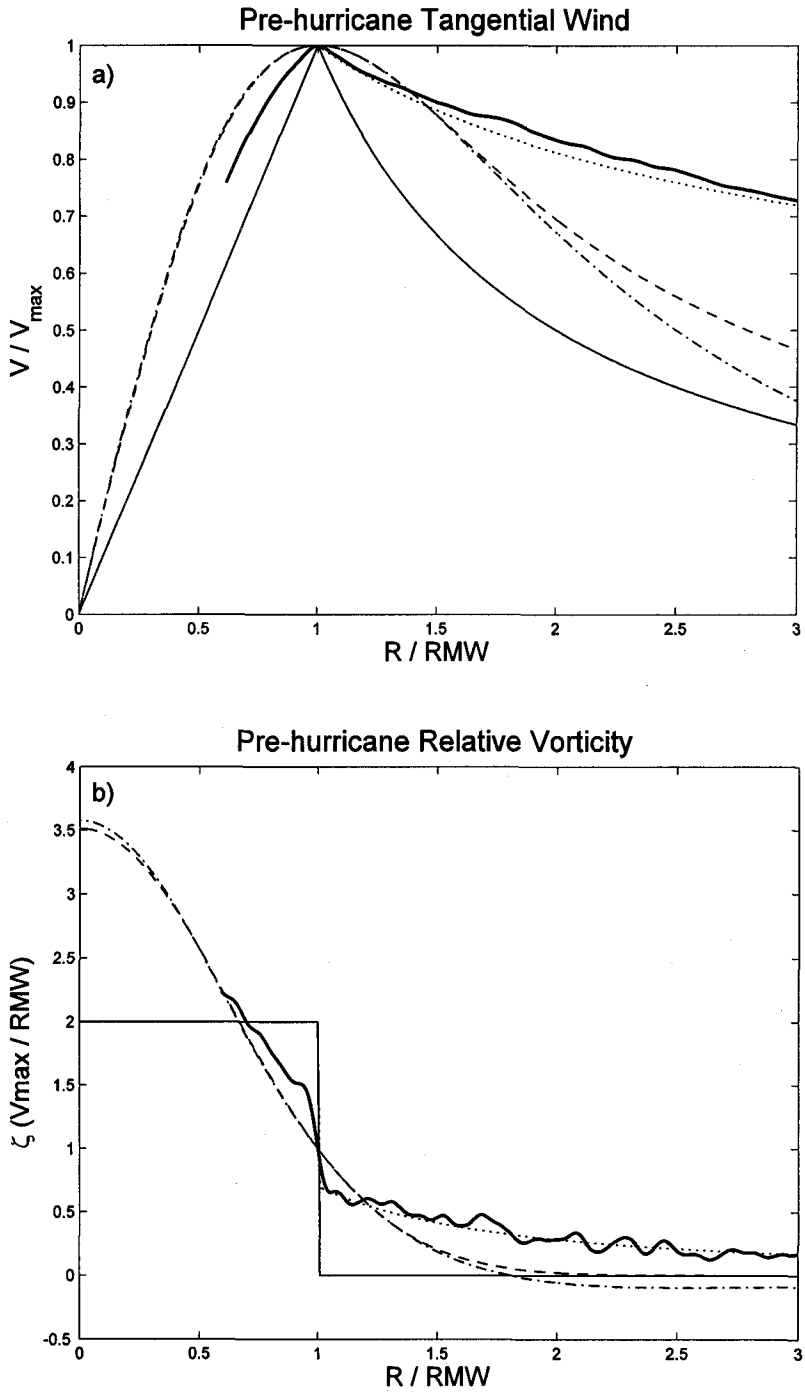

Figure 4.3. Composite non-dimensional radial profiles of observed pre-hurricane (a) tangential velocity and (b) relative vorticity (thick-solid) compared with equivalent idealized radial profiles for Rankine (thin solid line), Gaussian (dashed line) and J (dash-dotted line) vortices, in addition to the best-fit modified Rankine (dotted line) vortex (α=0.30).

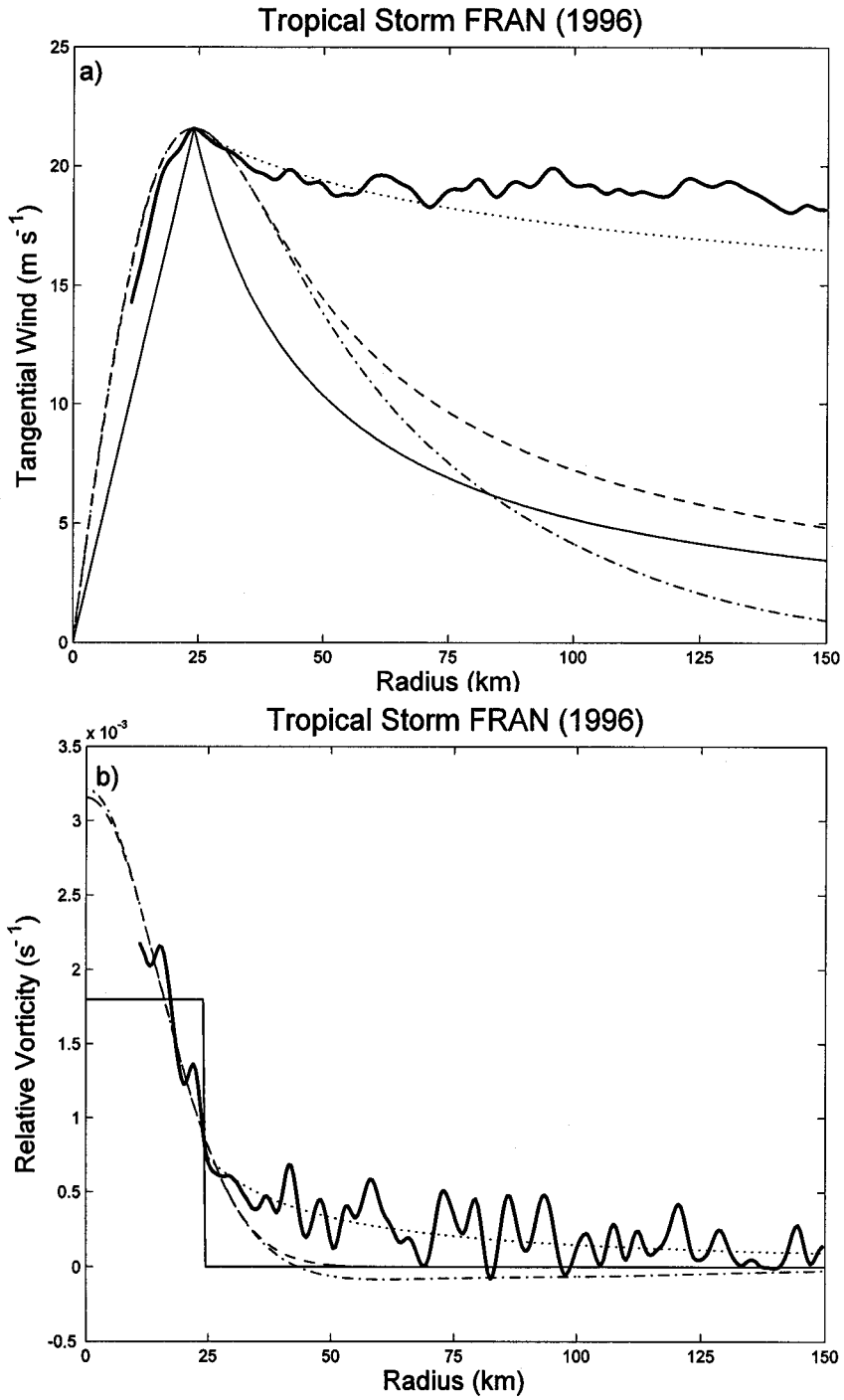

Figure 4.4. Estimated azimuthal mean radial profiles of (a) tangential wind speed and (b) relative vorticity from observations of tropical storm Fran during 0506-1243Z on 30 August 1996 (solid line), compared with equivalent idealized Rankine (thin solid line), Gaussian (dashed line) and J (dash-dotted line) ideal vortices, in addition to the best-fit modified Rankine vortex (dotted line, α=0.15).

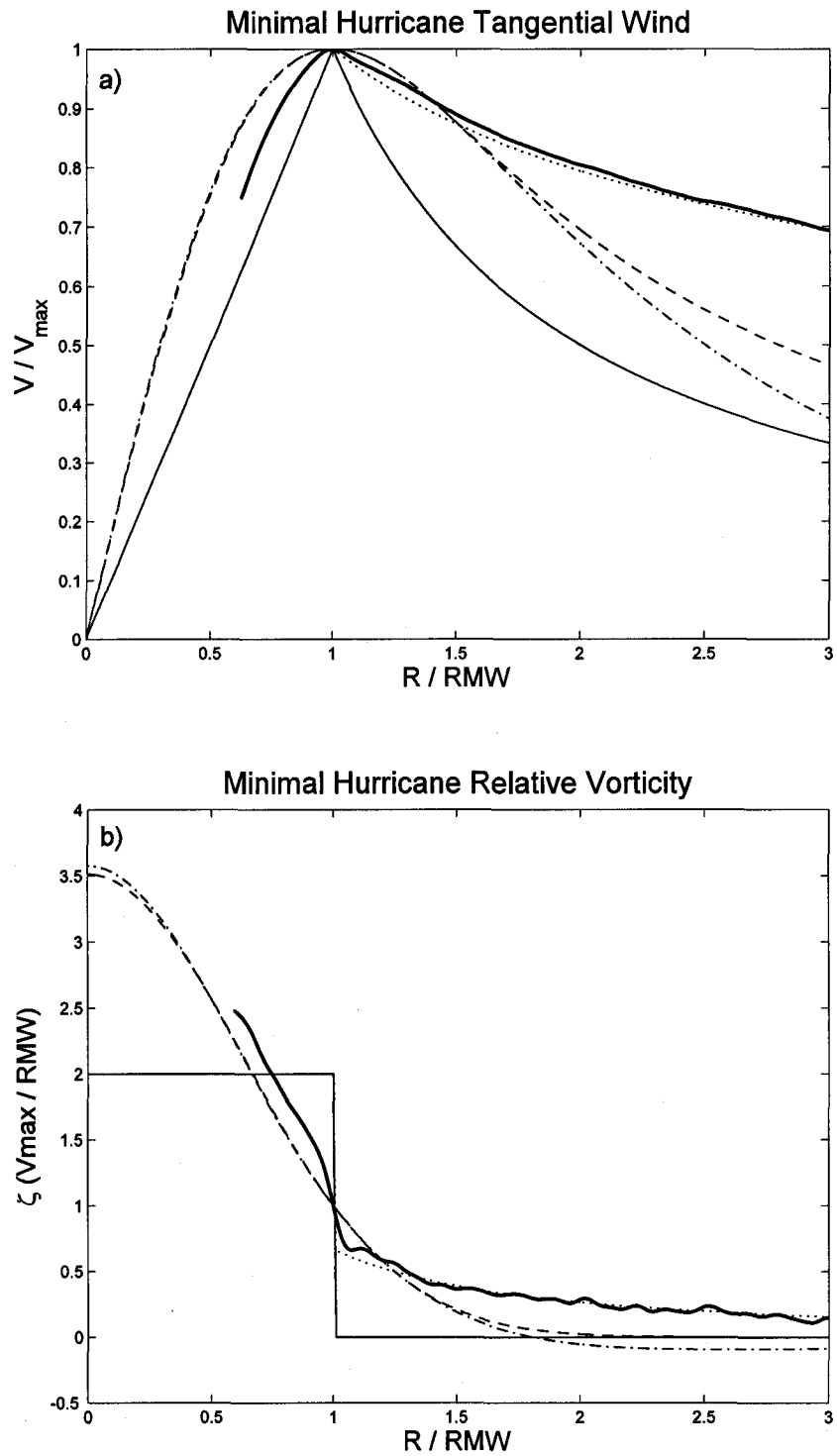

Figure 4.5. Same as Fig. 4.3 except for minimal hurricanes (α=0.35).

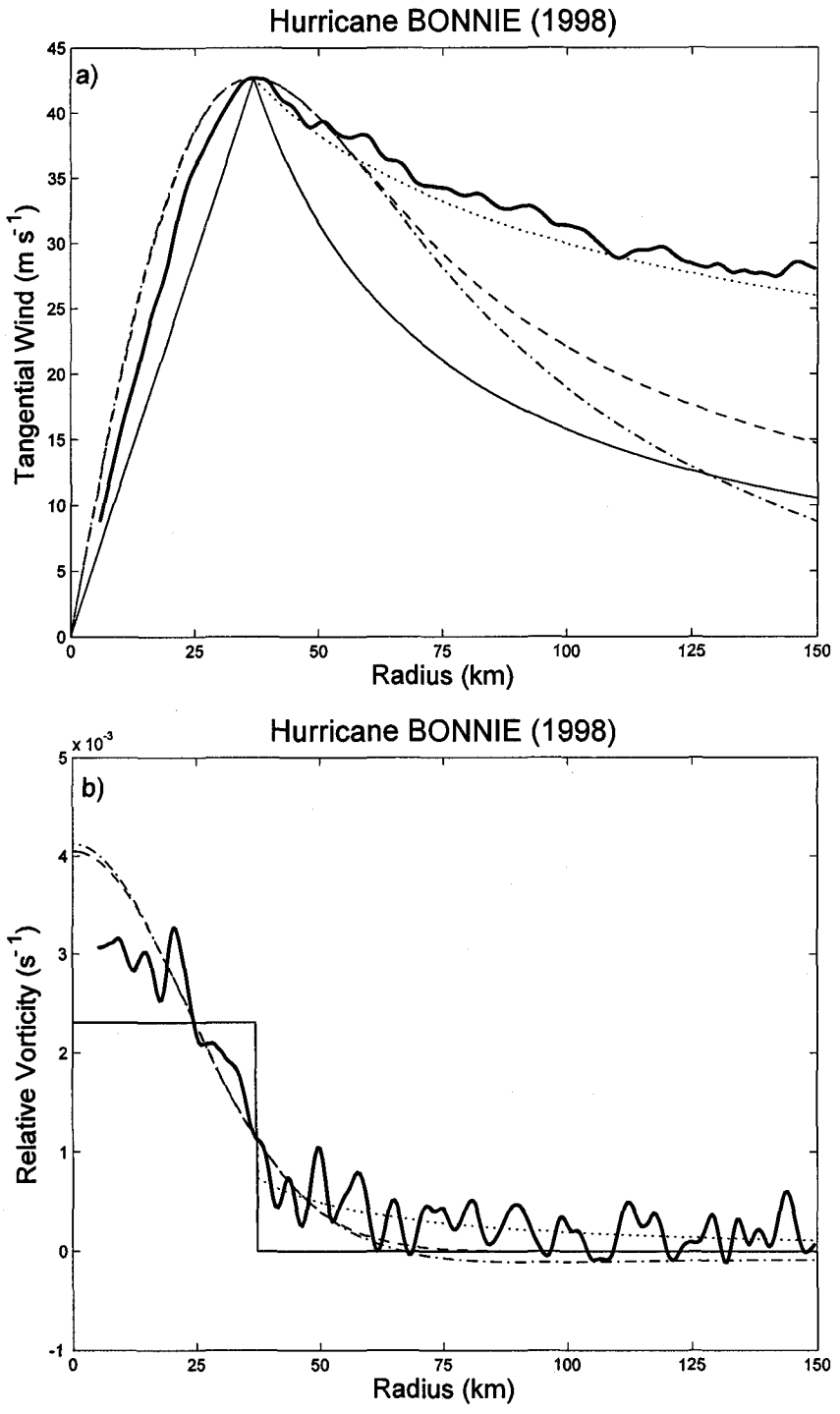

Figure 4.6. Same as Fig. 4.4 except for hurricane Bonnie during 0257-0538Z on 23 August 1998 and α=0.35.

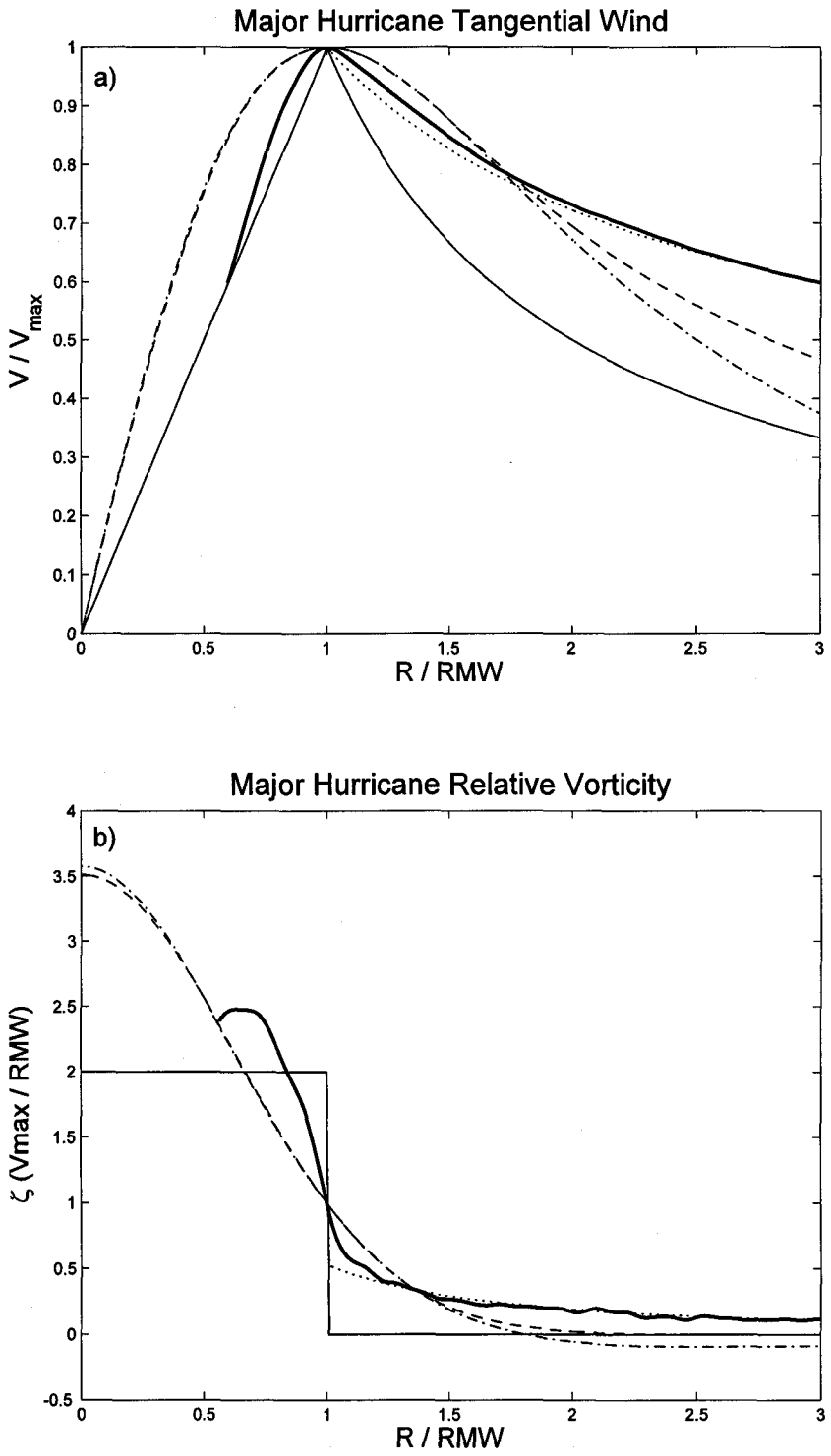

Figure 4.7. Same as Fig. 4.3 except for major hurricanes (α=0.48).

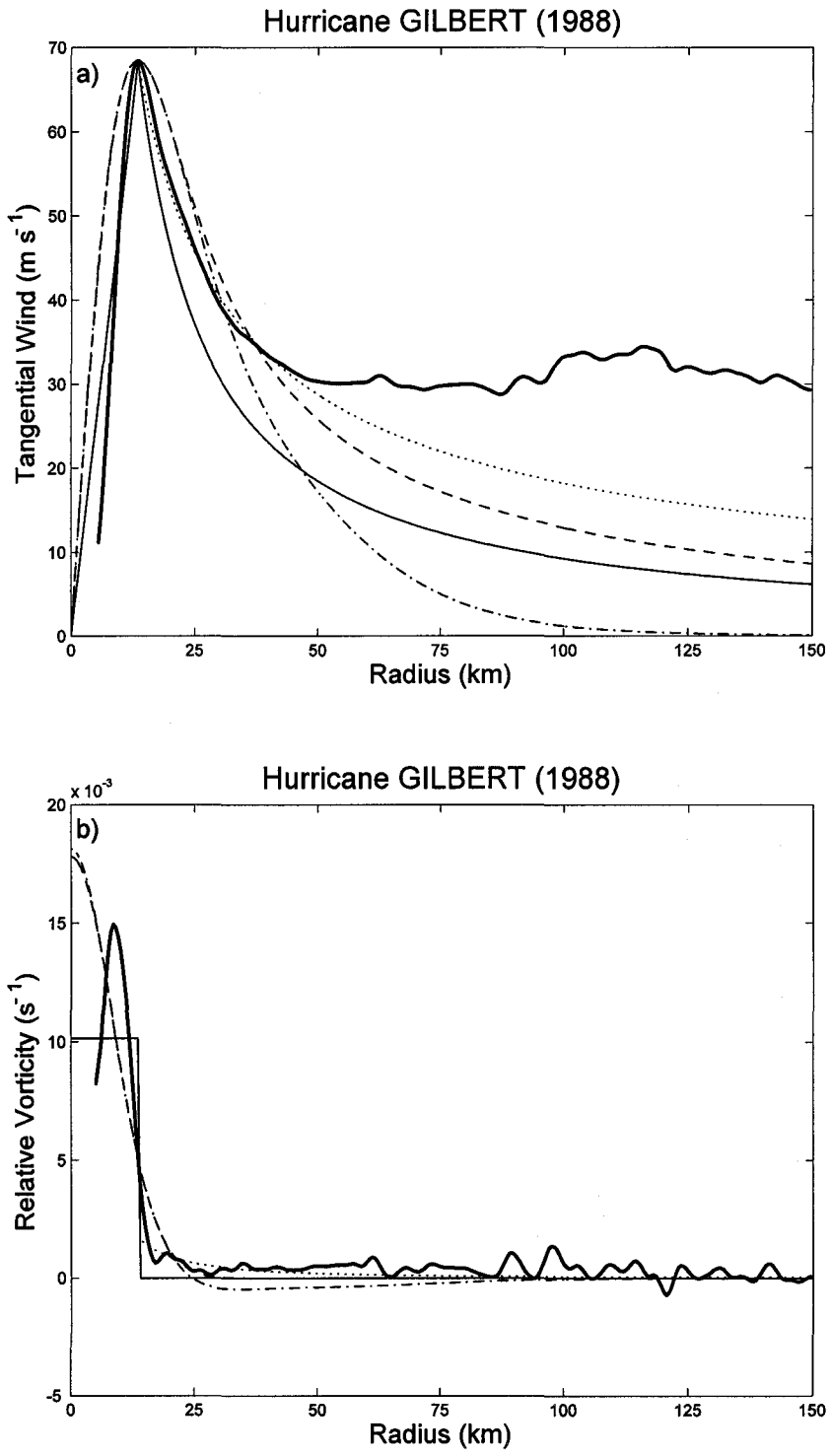

Figure 4.8. Same as Fig. 4.4 except for hurricane Gilbert during 1854-2053Z on 13 September 1988 and α=0.67.

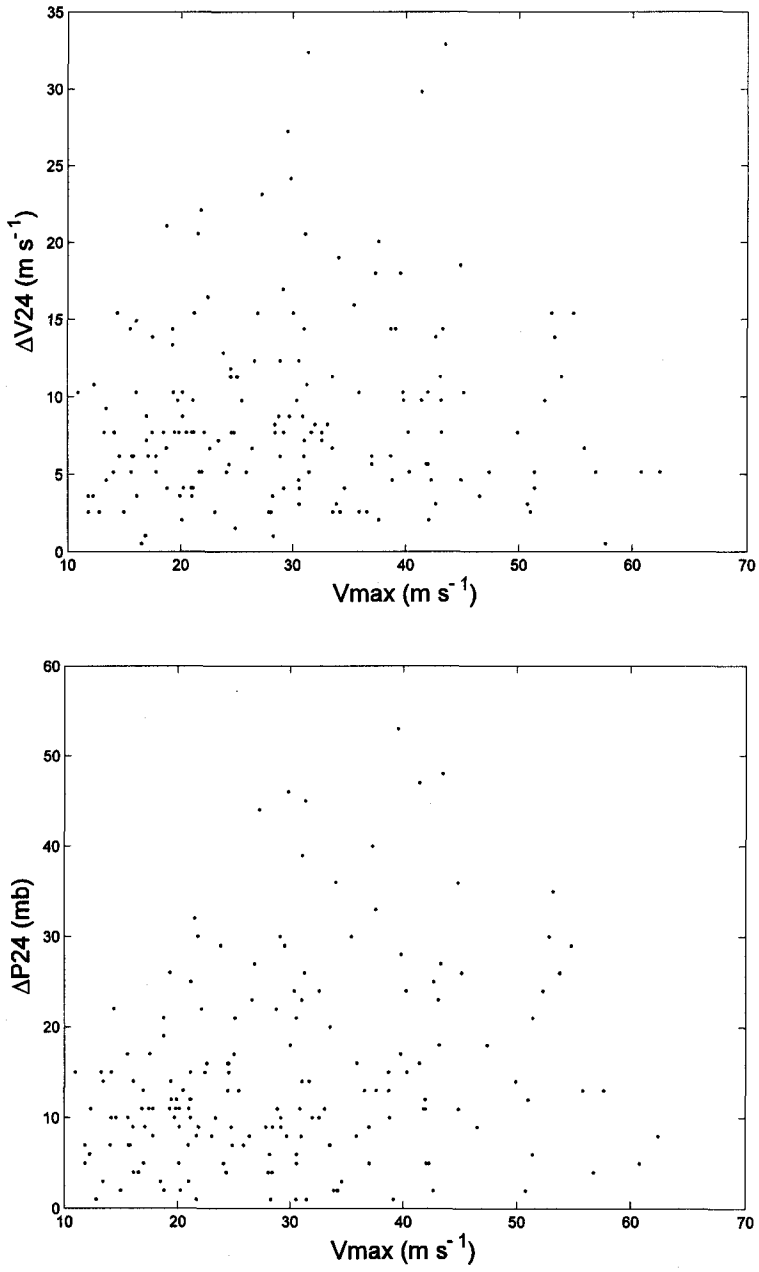

Figure 5.1. a) Scatter diagram of flight-level maximum azimuthal-mean tangential velocity (V_{max}) and the 24-hour maximum surface wind speed increase (ΔV_{24}) from the NHC best-track data set. b) Same as a), except for 24-hour central pressure fall (ΔP_{24}). The sample is restricted to intensifying cases only (176 total).

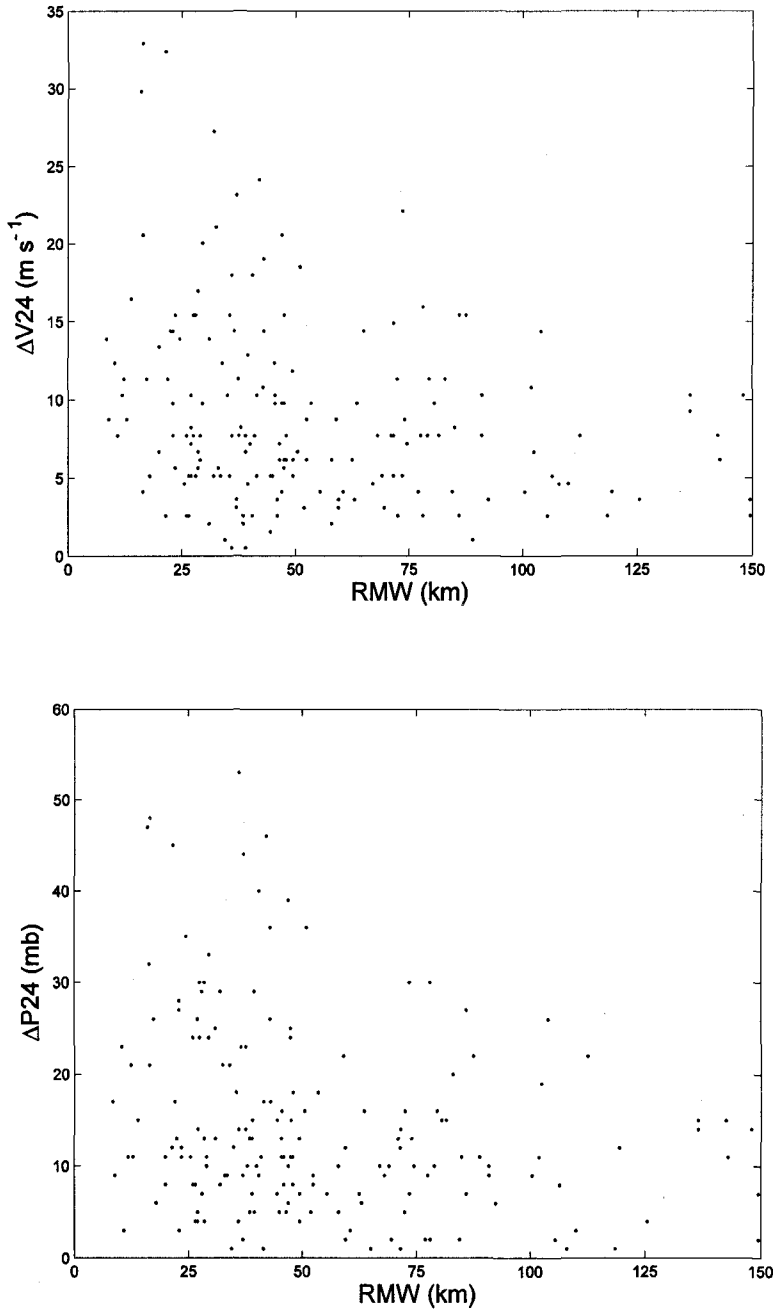

Figure 5.2. a) Scatter diagram of radius of maximum azimuthal-mean tangential velocity (RMW) and the 24-hour maximum surface wind speed increase (ΔV_{24}) from the NHC best-track data set. b) Same as a), except for 24-hour central pressure fall (ΔP_{24}). The sample is restricted to intensifying cases (176 total).

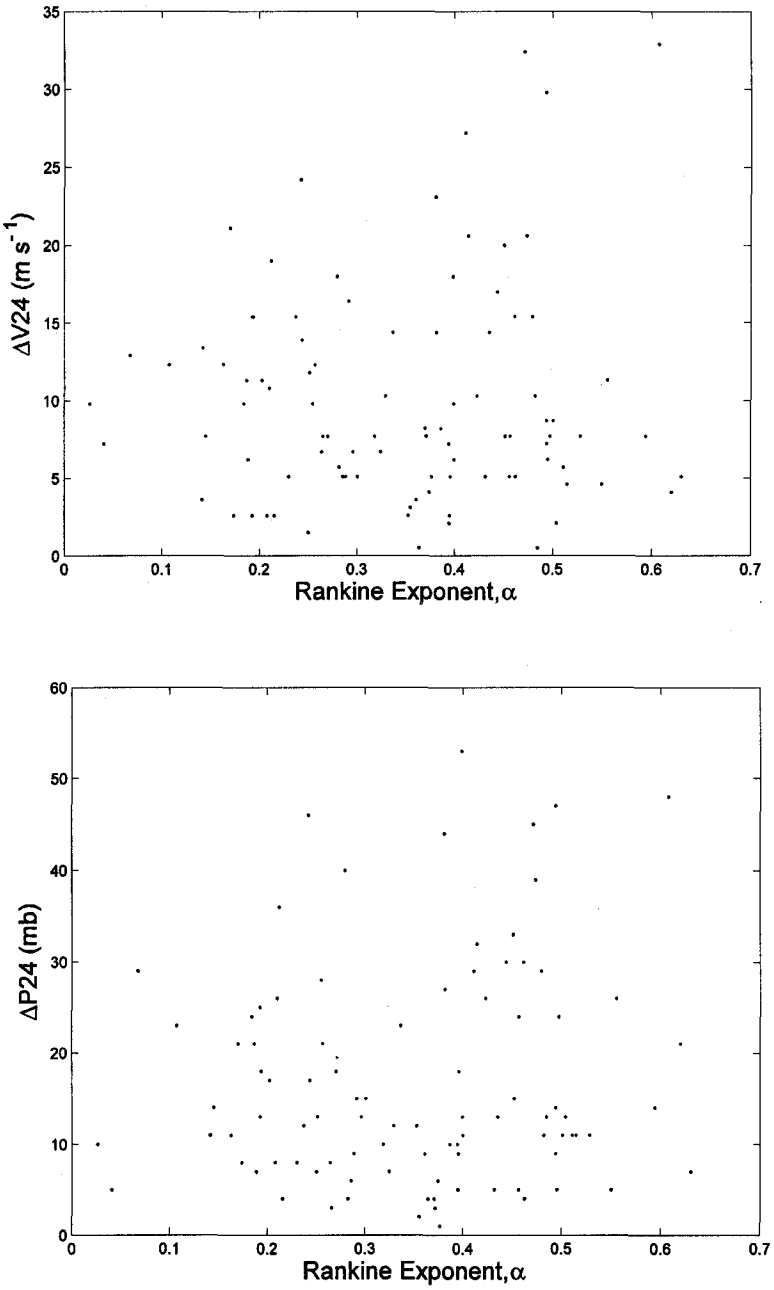

Figure 5.3. a) Scatter diagram of modified Rankine decay exponent (α) and the 24-hour maximum surface wind speed increase (ΔV_{24}) from the NHC best-track data set. b) Same as a), except for 24-hour minimum central pressure fall (ΔP_{24}). The sample is restricted to intensifying cases with RMW within 50 km (94 total).

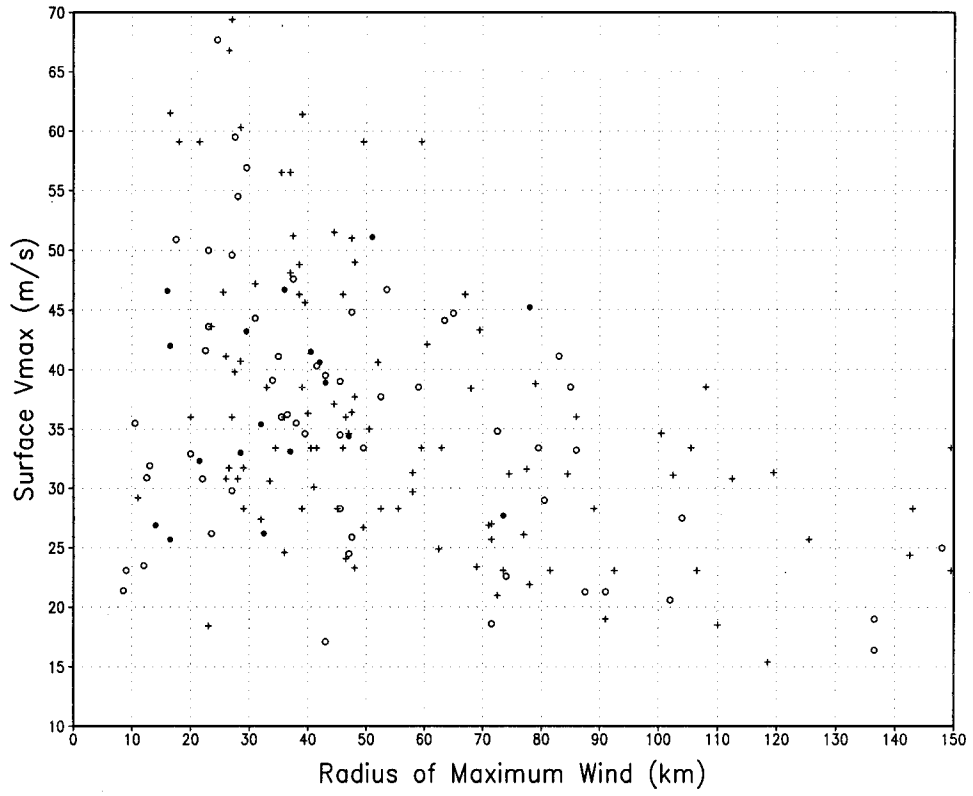

Figure 5.4. Scatter diagram of best-track maximum surface wind speed (V_m) and the approximate radius of maximum wind (RMW) stratified into three intensification classes defined by ranges (see text) in the 24-hour maximum surface wind speed increase (ΔV_{24}): *rapid* (solid circles), *moderate* (open circles) and *slow* (cross-hairs) (94 total).

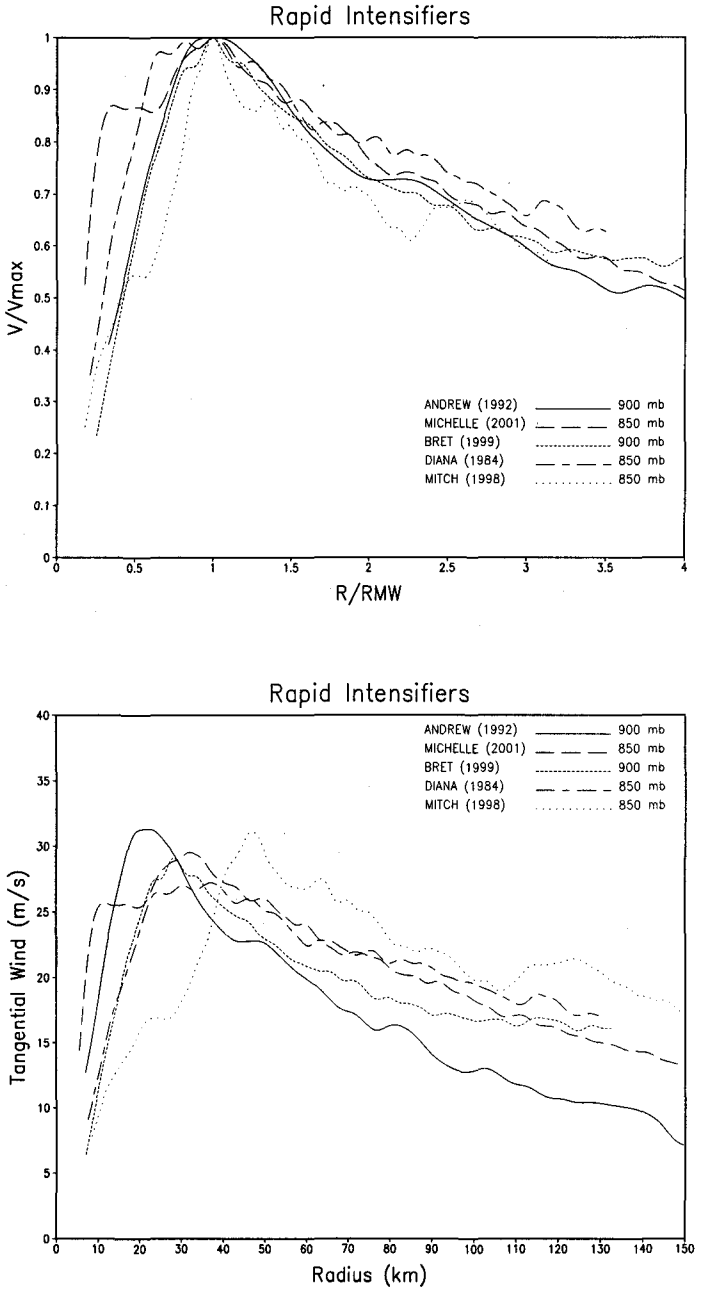

Figure 5.5. a) Radial profiles of azimuthal-mean tangential wind for five storms of minimum hurricane intensity near the beginning of their most rapid 24-hour intensification period displayed in: a) non-dimensional form out to four RMW distances b) dimensional form out to 150 km.

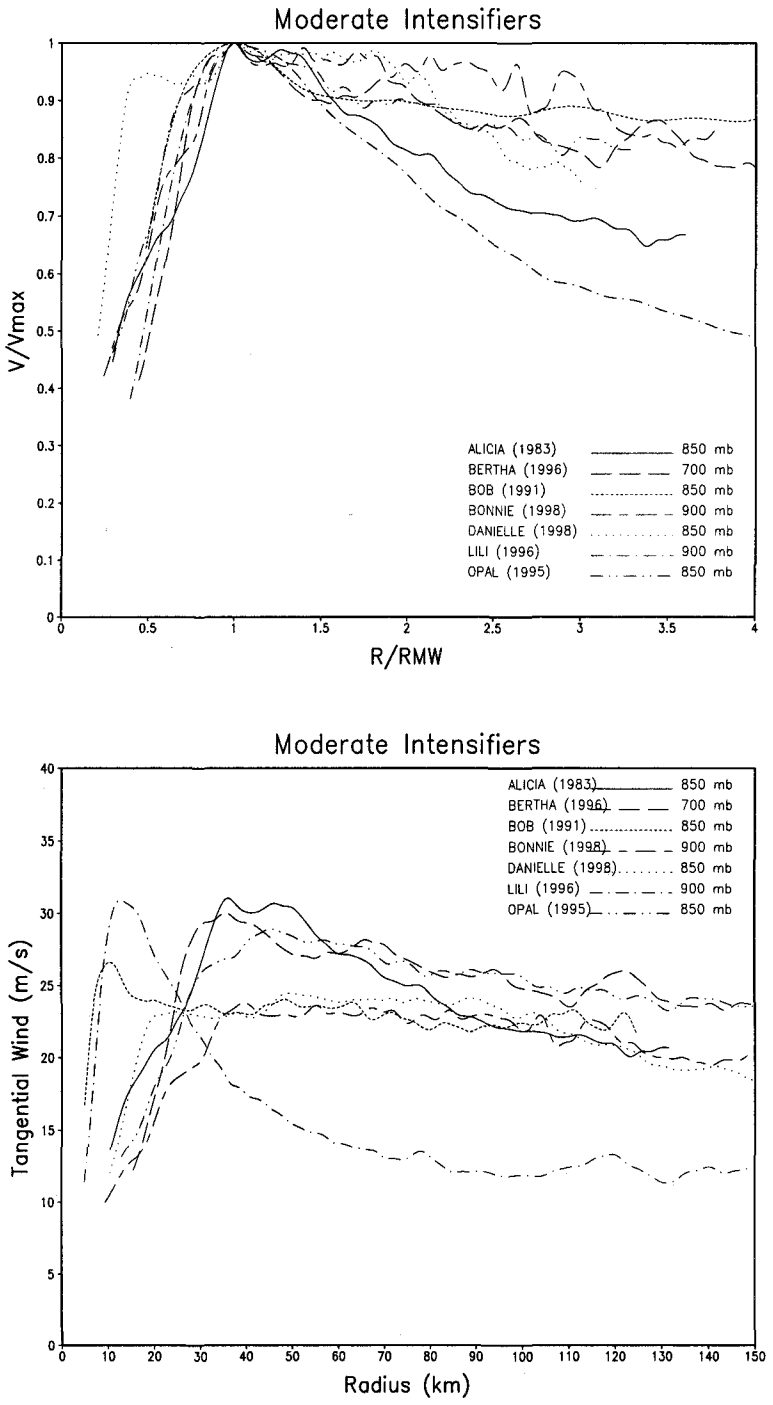

Figure 5.6. a) Same as Fig. 5.5, except for seven moderately intensifying storms.

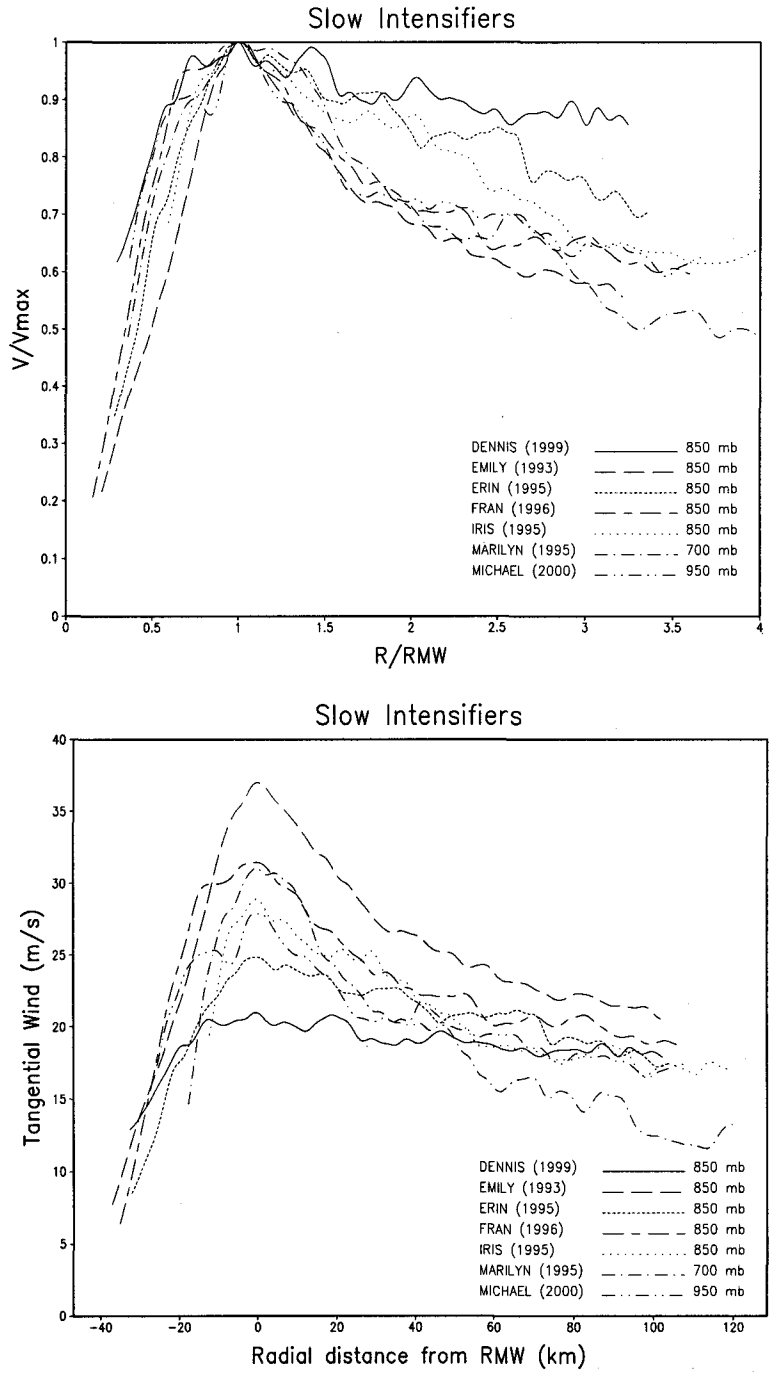

Figure 5.7. Same as Fig. 5.5, except for seven slowly intensifying storms.

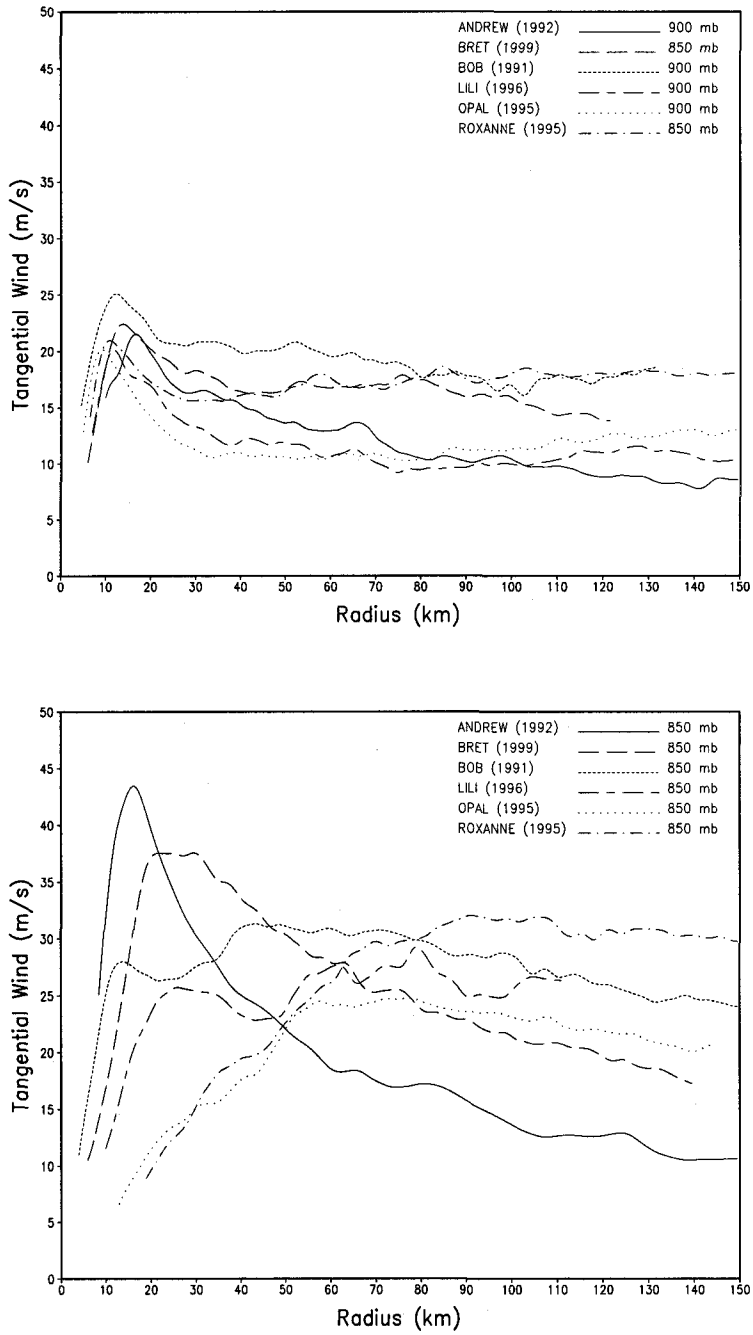

Figure 5.8. Radial profile of azimuthal-mean tangential velocity for six a) tropical storms with very small RMW (< 20 km) and b) the same six storms approximately 24 hours later, two of which rapidly intensified (Andrew and Bret) while the others intensified at a slower rate.

LIST OF ABBREVIATIONS AND SYMBOLS

α:	Tangential wind decay exponent for a modified Rankine vortex
P_c:	Minimum central sea-level pressure
RMW:	Radius of maximum azimuthal-mean tangential wind speed
V_{max}:	Maximum azimuthal-mean tangential wind speed
V_m:	Maximum surface wind speed
ΔV_{24}:	Future 24-hour increase in V_m
ΔP_{24}:	Future 24-hour increase in P_c

REFERENCES

Anthes, R. A., 1982: Tropical cyclones: Their evolution, structure and effects. *Meteor. Monogr.,*41., Amer. Meteor. Soc., Boston, MA 02108, 208 pp.

Batchelor, G. K., 1967: *"An introduction to fluid dynamics".* Cambridge University Press, London and New York, 615 pp.

Bender, M. A., R. J. Ross, R. E. Tuleya, and Y. Kurihara, 1993: Improvements in tropical cyclone track and intensity forecasts using the GFDL initialization system. *Mon. Wea. Rev.,* **121**, 2046-2061.

Black, P. G. and L. K. Shay, 1998: Observations of tropical cyclone intensity change due to air-sea interaction processes. Preprints, *Symp. on Tropical Cyclone Intensity Change*, Phoenix, AZ, Amer. Meteor. Soc., 161-168.

Bosart, L. F., C. S. Velden, W. E. Bracken, J. Molinari, P. G. Black, 2000: Environmental influences on the rapid intensification of Hurricane Opal (1995) over the Gulf of Mexico. *Mon. Wea. Rev.,* **128** 322-352.

Brand, S., 1973: Rapid intensification and low-latitude weakening of tropical cyclones of the western North Pacific ocean. *J. Appl. Meteor.,* **12**, 94-103.

Braun, S. A., M. T. Montgomery, and Z. Pu, 2003: High-resolution simulation of Hurricane Bonnie (1998). Part I: The organization of vertical motion. *J. Atmos. Sci.,* Submitted to CAMEX special issue.

Briggs, R. J., J. D. Daugherty and R. H. Levy, 1970: Role of Landau damping in crossed-field electron beams and inviscid shear flow.

Phys. Fluids, 13, 421-432.

Callaghan, J. and R. K. Smith, 1998: The relationship between maximum surface wind speeds and the central pressure in tropical cyclones. *J. Aust. Meteor. Soc.*, 47, 191-202.

Croxford, M. and G. M. Barnes, 2002: Inner core strength of Atlantic tropical cyclones. *Mon. Wea. Rev.*, 130, 127-139.

DeMaria, M. and J. Kaplan, 1994: A statistical hurricane intensity prediction scheme (SHIPS) for the Atlantic Basin. *Wea. Forecasting*, 9, 209-220.

DeMaria, M. and J. Kaplan, 1999: An updated statistical intensity prediction scheme (SHIPS) for the Atlantic and eastern North Pacific basins. *Wea. Forecasting*, 14, 326-337.

Depperman, C. E., 1947: Notes on the origin and structure of Philippine typhoons. *Bull. Amer. Meteor. Soc.*, 28, 399-404.

Eliassen, A., 1951: Slow thermally or frictionally controlled meridional circulation in a circular vortex. *Astrophys. Norv.*, 5, 19-60.

Emanuel, K. A. and M. Fantini, A. J. Thorpe, 1987: Baroclinic instability in an environment of small stability to slantwise moist convection. Part I: Two-dimensional models. *J. Atmos. Sci.*, 44, 1559-1573.

Frank, W. M., 1977: The structure and energetics of the tropical cyclone I. Storm structure. *Mon. Wea. Rev.*, 105, 1119-1135.

Franklin, J. L., S. J. Lord, S. E. Feuer, and F. D. Marks, Jr., 1993: The kinematic structure of hurricane Gloria (1985) determined from nested analyses of dropwindsonde and Doppler radar data. *Mon. Wea. Rev.*, 121, 2433-2451.

Gent, P. R., and J. C. McWilliams, 1986: The instability of barotropic circular vortices. Geophys. Astrophys. Fluid Dyn., **35**, 209-233.

Gray, W. M. and D. J. Shea, 1973: The hurricane's inner core region. II. Thermal Stability and Dynamic Characteristics. *J. Atmos. Sci.*, **30**, 1565-1576.

Holliday, C.R., and A.H. Thompson, 1979: Climatological characteristics of rapidly intensifying typhoons. *Mon. Wea. Rev.*, **107**, 1022-1035.

Hong, X., S. W. Chang, S. Raman, L. K. Shay, and R. Hodur, 2000: The interaction between Hurricane Opal (1995) and a warm-core ring over the Gulf of Mexico. *Mon. Wea. Rev.,* **128** 1347-1365.

Hoskins, B.J., M. E. McIntyre and A. W. Robertson, 1985: On the use and significance of isentropic potential vorticity maps. *Quart. J. Roy. Meteor. Soc.*, **111**, 877-946.

Hughes, L. A., 1952: On the low-level wind structure of tropical storms. *J. Meteor.*, **9**, 422-428.

Jones, S.C., 1995: The evolution of vortices in vertical shear. I: Initially barotropic vortices. *Quart. J. Roy. Meteor. Soc.*, **121**, 821-851.

Jones, S.C., 2000: The evolution of vortices in vertical shear. II: Large-scale asymmetries. *Quart. J. Roy. Meteor. Soc.*, **126**, 3137-3159.

Jorgensen, D. P., 1984: Mesoscale and convective-scale characteristics of mature hurricanes. Part I: General observations by research aircraft. *J. Atmos. Sci.*, **41**, 1268-1285.

Kaplan, J. and M. DeMaria, 2003: Large-scale characteristics of rapidly intensifying tropical cyclones in the North Atlantic basin. *Wea. Forecasting*, **18**, 1093-1108.

Kossin, J. P. and M. D. Eastin 2001: Two distinct regimes in kinematic and thermodynamic structure of the hurricane eye and eyewall. *J. Atmos. Sci.*, **48**, 1079-1090.

Kurihara, Y., R. E. Tuleya, and M. A. Bender 1998: The GFDL hurricane prediction system and its performance in the 1995 hurricane season. *Mon. Wea. Rev.*, **126**, 1306-1322.

Malkus, J. S. and H. Riehl, 1960: On the dynamics and energy transformation in steady-state hurricanes. *Tellus*, **12**, 1-20.

McWilliams, J. C., L. P. Graves, and M. T. Montgomery, 2003: A formal theory for vortex Rossby waves and vortex evolution. *Geophys. Astrophys. Fluid Dynamics*, **97**, 275 – 309.

Merrill, R. T., 1984: A comparison of large and small tropical cyclones. *Mon. Wea. Rev.*, **112**, 1408-1418.

Miller, B. I., 1967: Characteristics of hurricanes. *Science*, **157**, 1389-1399.

Montgomery, M. T. and B. F. Farrell, 1992: Polar Low Dynamics. *J. Atmos. Sci.*, **49**, 2484-2505.

Moller, D. J. and M. T. Montgomery, 2000: Tropical cyclone evolution via potential vorticity anomalies in a three-dimensional balance model. *J. Atmos. Sci.*, **57**, 3366-3387.

Montgomery, M.T. and R.J. Kallenbach, 1997: A theory of vortex Rossby-waves and its application to spiral bands and intensity changes in hurricanes. *Quart. J. Roy. Meteor. Soc.*, **123**, 435-465.

Montgomery, M.T., V. A. Vladimirov and P. V. Denissenko, 2002: An experimental study on hurricane mesovortices. *J. Fluid Mech.*, **471**, 1-32.

OFCM, 1993: National Hurricane Operations Plan, 125 pp. [Available from Office of the Federal Coordinator for Meteorological Services and Supporting Research, Suite 1500, 8455 Colesville Rd., Silver Spring, MD 20910.]

Ooyama, K., 1969: Numerical simulation of the life cycle of tropical cyclones. *J. Atmos. Sci.*, **26**, 3-40.

Orr, W. M., 1907: The stability or instability of the steady motions of a perfect liquid and of a viscous liquid. *Proc. Roy. Irish Acad.*, **A27**, 9-138.

Pearce, R. P., 1992: A critical review of progress in tropical cyclone physics including experimentation with numerical models. *ICSU/WMO International Symposium on Tropical Disasters*, Beijing, China, 45-59.

Petrova, L. I., 1995: Radial structure of tangential wind in a tropical cyclone as derived from observational data. *Russian Meteorology and Hydrology*, **3**, 1-8.

Reasor, P. D., M. T. Montgomery, F. D. Marks, and J. F. Gamache, 2000: Low wavenumber structure and evolution of the hurricane inner core observed by airborne dual-Doppler radar. *Mon. Wea. Rev.*, **128**, 1653-1680.

Reasor, P. D. and M. T. Montgomery, 2001: Three-dimensional alignment and corotation of weak TC-like vortices via linear vortex Rossby waves. *J. Atmos. Sci.*, **58**, 2306-2330.

Persing, J. and M. T. Montgomery, 2003: Hurricane superintensity. *J. Atmos. Sci.*, **60**, 2349-2371.

Reasor, P. D., M. T. Montgomery and L. D. Grasso, 2004: A new look at the problem of tropical cyclones in vertical shear flow: Vortex resiliency. *J. Atmos. Sci.*, **61**, 3-22.

Riehl, H., 1954: *Tropical Meteorology*. New York, McGraw-Hill, Chapter 11.

Riehl, H., 1963: Some relations between wind and thermal structure of steady state hurricanes. *J. Atmos. Sci.*, **20**, 276-287.

Rotunno, R. and K. A. Emanuel, 1987: An air-sea interaction theory for tropical cyclones. Part II: Evolutionary study using a nonhydrostatic axisymmetric numerical model. *J. Atmos. Sci.*, **44**, 542-561.

Samsury, C. E. and E. J. Zipser, 1995: Secondary wind maxima in hurricanes: airflow and relationship to rainbands. *Mon. Wea. Rev.*, **123**, 3502-3517.

Schecter, D. A., M. T. Montgomery and P. D. Reasor, 2002: A theory for the vertical alignment of a quasi-geostrophic vortex. *J. Atmos. Sci.*, **59**, 150-168.

Schecter, D. A. and M. T. Montgomery, 2003: On the symmetrization rate of an intense geophysical vortex. *Dyn. Atmos. Oceans*, **37**, 55-88.

Schecter, D. A. and M. T. Montgomery, 2004: Damping and pumping of a vortex Rossby wave in a monotonic cyclone: Critical layer stirring versus inertia-buoyancy wave emission. *Phys. Fluids*, in press.

Schubert, W. H. and M. T. Montgomery, R. K. Taft, T. A. Guinn, S. R. Fulton, J. P. Kossin, and J. P. Edwards, 1999: Polygonal eyewalls, asymmetric eye contraction, and potential vorticity mixing in hurricanes. *J. Atmos. Sci.*, **56**, 1197-1223.

Schubert, W. H. and J. J. Hack, 1982: Inertial Stability and Tropical Cyclone Development. *J. Atmos. Sci.*, **39**, 1687-1697.

Shapiro, L.J. and H.E. Willoughby, 1982: The response of balanced hurricanes to local sources of heat and momentum. *J. Atmos. Sci.*, **39**, 378-394.

Shapiro, L. J., and M. T. Montgomery, 1993: A three-dimensional balance theory for rapidly rotating vortices. *J. Atmos. Sci.*, **50**, 3322-3335.

Shapiro, L. J., and J. L. Franklin, 1995: Potential vorticity in hurricane Gloria. *Mon. Weather Rev.*, **123**, 1465-1475.

Shay, L. K., G. J. Goni, and P. G. Black, 2000: Effects of a warm oceanic feature on Hurricane Opal. *Mon. Wea. Rev.,* **128** 1366-1383.

Shea, D. J. and W. M. Gray, 1973: The hurricane's inner core region. I. Symmetric and Asymmetric Structure. *J. Atmos. Sci.*, **30**, 1544-1564.

Sheets, R. C., 1980: Some aspects of tropical cyclone modification. *Aust. Meteor. Mag.*, **27**, 259-280.

Smith, R. K., 1990: A numerical study of tropical cyclone motion using a barotropic model. I: The role of vortex asymmetries. *Quart. J. Roy. Meteor. Soc.*, **116**, 337-362.

Stossmeister, G. J. and G. M. Barnes, 1992: The development of a second circulation center with tropical storm Isabel (1985). *Mon. Wea. Rev.,* **128**, 685-697.

Thomson, W. W., 1887: Stability of fluid motion: Rectilinear motion of viscous fluid between two parallel plates. *Philos. Mag.*, **24**, 188 – 196.

Thorpe, A. J., 1985: Diagnosis of balanced vortex structure using potential

vorticity. *J. Atmos. Sci.*, **42**, 397-406.

Wang, Y., and G. J. Holland, 1996: Tropical cyclone motion and evolution in vertical shear. *J. Atmos. Sci.*, **53**, 3313-3332.

Weatherford, C. L., 1989: The structural evolution of typhoons. Atmos. Sci. Paper, No. 446, Dept. Atmos. Sci. Colorado State University, 198 pp.

Willoughby, H.E., 1979: Forced secondary circulations in hurricanes. *J. Geophys. Res.*, **47**, 242-264.

Willoughby, H. E., J. A. Clos and M. G. Shoreibah, 1982: Concentric eyewalls, secondary wind maxima, and the evolution of the hurricane vortex. *J. Atmos. Sci.*, **39**, 395-411.

Willoughby, H. E. and M. B. Chelmow, 1982: Objective determination of hurricane tracks from aircraft observations. *Mon. Wea. Rev.*, **110**, 1298-1305.

Willoughby, H. E., 1990a: Temporal changes of the primary circulation in tropical cyclones. *J. Atmos. Sci.*, **47**, 242-264.

Willoughby, H. E., 1990b: Gradient balance in tropical cyclones. *J. Atmos. Sci.*, **47**, 265-274.

Willoughby, H. E. and M. E. Rahn, 2004: Parametric representation of the primary hurricane vortex. Part I: Observations and evaluation of the Holland (1980) model. *Mon. Wea. Rev.*, submitted for publication.